

NASA TECHNICAL NOTE



NASA TN D-6842

6.1

NASA TN D-6842



0133658

TECH LIBRARY KAFB, NM

LOAN COPY: RETURN TO
AFWL (DOUL)
KIRTLAND AFB, N. M.

CYCLIC OXIDATION OF
COBALT-CHROMIUM-ALUMINUM-YTTRIUM
AND ALUMINIDE COATINGS
ON IN-100 AND VIA ALLOYS
IN HIGH-VELOCITY GASES

by Daniel L. Deadmore
Lewis Research Center
Cleveland, Ohio 44135





0133658

1. Report No. NASA TN D-6842	2. Government Accession No.	3. Recipient's Catalog No.	
4. Title and Subtitle CYCLIC OXIDATION OF COBALT-CHROMIUM-ALUMINUM-YTTRIUM AND ALUMINIDE COATINGS ON IN-100 AND VIA ALLOYS IN HIGH-VELOCITY GASES		5. Report Date July 1972	
		6. Performing Organization Code	
7. Author(s) Daniel L. Deadmore		8. Performing Organization Report No. E-6809	
		10. Work Unit No. 134-03	
9. Performing Organization Name and Address Lewis Research Center National Aeronautics and Space Administration Cleveland, Ohio 44135		11. Contract or Grant No.	
		13. Type of Report and Period Covered Technical Note	
12. Sponsoring Agency Name and Address National Aeronautics and Space Administration Washington, D. C. 20546		14. Sponsoring Agency Code	
		15. Supplementary Notes	
16. Abstract <p>Embedded-alumina-particle aluminide (EAPA) coated and CoCrAlY coated IN-100 and NASA-TRW-VIA specimens were cyclically oxidation tested in a high-velocity (approximately Mach 1) gas flame at 1093^o C (2000^o F). The EAPA coatings on both alloys performed very similarly to commercial pack aluminide coatings with respect to weight change and thermal fatigue cracking. The CoCrAlY coating on IN-100 had weight changes similar to commercial pack aluminide coatings but no thermal fatigue cracks appeared at 300 hours. The CoCrAlY coating on VIA performed significantly better than the commercial aluminide coatings, providing oxidation protection (based on weight change) to 450 hours and thermal fatigue crack prevention to at least 600 hours.</p>			
17. Key Words (Suggested by Author(s)) Oxidation; High-velocity gases; Nickel base superalloys; Aluminide coatings; CoCrAlY coatings		18. Distribution Statement Unclassified - unlimited	
19. Security Classif. (of this report) Unclassified	20. Security Classif. (of this page) Unclassified	21. No. of Pages 35	22. Price* \$3.00

**CYCLIC OXIDATION OF COBALT-CHROMIUM-ALUMINUM-YTTRIUM
AND ALUMINIDE COATINGS ON IN-100 AND VIA
ALLOYS IN HIGH-VELOCITY GASES**

by Daniel L. Deadmore

Lewis Research Center

SUMMARY

Nickel base superalloys IN-100 and NASA-TRW-VIA specimens were contractually coated with an embedded-alumina-particle aluminide (EAPA) composition by a modified pack cementation process and with a CoCrAlY composition by physical vapor deposition.

All specimens were oxidation tested at 1093^o C (2000^o F) in a high-velocity gas flame (approximately Mach 1) under cyclic conditions. The EAPA coating on IN-100 provided oxidation protection (as measured by the time to show a maximum weight gain and a turn-around in weight change behavior) for 100 to 150 hours and on VIA for 50 to 100 hours. This is about the same time as commercial aluminide coatings without embedded alumina. Thermal fatigue cracking behavior was also similar. The CoCrAlY coating on IN-100 was protective for 150 to 160 hours. While this protection was similar to commercial pack aluminide coatings tested under the same conditions, the CoCrAlY coating on VIA was protective for at least 450 hours of such oxidation testing and prevented thermal fatigue crack formation up to at least 600 hours. This is a significant improvement over previously tested commercial coatings.

From metallographic, X-ray fluorescence, X-ray diffraction, microhardness, and electron microprobe results, the degradation of both types of coatings was shown to be primarily related to aluminum loss due to surface oxide spalling.

INTRODUCTION

Higher operating temperatures in aircraft gas turbine engines have created a greater need for long-life, high-temperature protective coatings. To meet this need, there has been a continued effort to improve the conventional aluminide coatings and to develop alternate coating approaches. Under Lewis Research Center sponsorship, alumi-

nide coatings have been developed in which very fine aluminum oxide particles are dispersed (ref. 1). Also, a compositional optimization of a CoCrAlY overlay coating, applied by physical vapor deposition, has been carried out (ref. 2). In each, promising systems were developed which, on the basis of the developer's test, offered greatly extended protection for nickel-based superalloy NASA-TRW-VIA as compared with currently used coatings.

The purpose of this study was to examine the oxidation resistance of these promising coatings under the same test conditions so as to compare their protective ability. By using a high-velocity-gas test facility, the data could also be compared with those obtained for a variety of commercial and experimental coatings previously evaluated. In addition, these coatings were examined not only on the VIA alloy, which is rich in refractory metals, but also on a commercial nickel turbine blade alloy, such as IN-100, in order to determine if a significant substrate effect is operative.

The coating/substrate systems were tested in the Lewis burner rig at 1093^o C (2000^o F) in high-velocity (approximately Mach 1) combustion gases using cycles of 1 hour at temperature and 3 minutes cooling to room temperature. Coating performance was primarily evaluated by visual, metallographic, and weight change data. These data were supplemented with X-ray diffraction (XRD), X-ray fluorescence (XRF), and electron microprobe (EMP) data to examine the influence of substrate chemistry on coating degradation.

MATERIALS AND TEST PROCEDURES

Specimens

The nominal compositions of the substrate alloys are: for IN-100, Ni-10Cr-15Co-5.6Al-3Mo-4.2Ti-1.0V and for VIA, Ni-6Cr-7Co-5Al-2Mo-1Ti-6W-9Ta-0.5Hf-0.5Nb-0.4Re. Both of the alloys were cast; then the groove and notch near the bottom of the bar were machined before coating. The test specimen geometry is shown in figure 1. This shape will be called the Lewis wedge bar specimen geometry. This designation is necessary, since comparison of our results with literature results, where a bow paddle geometry test specimen was used, will be made later. The exact shape of the bow paddle specimens can be found in reference 2.

Lewis wedge bar specimens of each alloy were coated by two NASA contractors. EAPA coating was applied by a dual-cycle, modified-pack-cementation, aluminizing process. Approximately 15 volume percent of 2-micrometer alumina particles were entrapped in the coating (ref. 1). The EAPA coating on VIA ranged in thickness from 0.0038 to 0.006 centimeter and on IN-100 from 0.001 to 0.0058 centimeter. The

CoCrAlY coating was applied by an electron-beam-heat-source, physical-vapor-deposition process (ref. 2). The deposited coating was nominally Co-22Cr-14Al-0.1Y. The CoCrAlY coating on VIA ranged in thickness from 0.0127 to 0.0162 centimeter, and on IN-100 from 0.0175 to 0.0225 centimeter. The coating thicknesses for both the EAPA and the CoCrAlY systems are each in the range in which they could be used commercially. Note, however, that the CoCrAlY system can be applied and used at about twice the thickness of the aluminide EAPA coating and of commercial aluminide coatings in current engine service. Other results of pretest examinations of the coated test specimens will be presented in the RESULTS AND DISCUSSION section.

High-Gas-Velocity Cyclic Oxidation

Figures 2(a) and (b) show an overall view and a schematic of the high-gas-velocity, natural-gas fueled burner rig used in the cyclic oxidation tests conducted in this study. Figure 2(c) is a photograph of the specimen holder. A detailed description of this apparatus is given in reference 3. The conditions of test operation for the high-gas-velocity burner rig are presented in table I. The gas velocity in the burner nozzle is Mach 1, but at the specimens it is slightly less. In each test cycle the specimens rotate in the air-rich natural gas combustion products for 1 hour with the sharply tapered edges of the specimens closest to the nozzle. At the end of the hour, the specimens are lowered into a high velocity (approximately Mach 1) cooling air blast for 3 minutes, which cools the specimens to room temperature. On heating, the specimens reached

TABLE I. - TYPICAL BURNER CONDITIONS FOR LEWIS HIGH-GAS-VELOCITY TESTER

Maximum specimen temperature, °C (°F)	1093 (2000)
Burner gas temperature, °C (°F)	1538 (2800)
Gas velocity	Mach 1
Burner pressure, MN/m ² (psia)	0.023 (33)
Specimen rotational speed, rpm	900
Burner airflow, kg/sec (lbm/sec)	0.45 (1.0)
Cooling airflow, kg/sec (lbm/sec)	0.23 (0.5)
Air to fuel ratio	20 to 30
Burner nozzle diameter, cm (in.)	5.1 (2.0)
Fuel	Natural gas
Time at temperature, hr	1
Time to heat specimens to temperature, min	1
Cooling time, min	3
Minimum cooling temperature	Room temperature
Distance, throat to specimen leading edge, cm (in.)	5.1 (2.0)

test temperature in 1 minute. Temperatures were measured using a slip ring and thermocouple arrangement connected to a dummy specimen in the rotating specimen holder assembly and were controlled by a stationary control thermocouple downstream of the test specimens. Temperature checks were made with a calibrated optical pyrometer. Specimen temperatures were maintained at $\pm 8^{\circ}\text{C}$ ($\pm 15^{\circ}\text{F}$).

Specimen Evaluation

Weight change. - The test specimens were weighted to the nearest 0.1 milligram before the test and after every 20 cycles of 1 hour duration. The difference between the initial and subsequent weight of the specimen is the weight change reported here. Up to 100 hours the results are the average of two specimens; above 100 hours the results are for a single specimen.

Visual change. - The test specimens were also examined visually under a low-power ($\times 30$ magnification) microscope at each 20-hour inspection. Photographs were taken at appropriate intervals.

X-ray diffraction. - At selected times, in-situ specimen surfaces were analyzed by X-ray diffraction using nickel-filtered copper K_{α} radiation (40 kV, 40 mA). The phases were identified by comparison with the ASTM X-Ray Data File. The area of the specimen studied was the flat side of the bar at 3.18 centimeters (1.25 in.) from the top of the bar (fig. 1), unless otherwise noted. This was in the zone which experienced the maximum temperature during test.

X-ray fluorescence. - At the same intervals and locations, the test specimen surfaces were analyzed by X-ray fluorescence to determine the changes in major substrate and coating-element concentration. The counts recorded for the analyzed elements were divided by the counts for the same elements from the bare substrate. This approach is more useful for the aluminide conversion coatings than for the CoCrAlY overlay coating where lesser amounts of the substrate elements can be expected to be observed in the coating surface.

Metallography. - Specimens, both before and after testing, were sectioned for metallographic examination. An arbitrarily chosen coated specimen was sectioned at every 1.27 centimeters (0.5 in.) starting from the top end of the bar for the purpose of metallographically measuring both the vertical and longitudinal coating thickness distribution. The mounted sections were polished and etched with a solution of 33 parts acetic acid, 33 parts glycerin, 33 parts nitric acid, and 1 part hydrofluoric acid. The total thickness of the coatings and the outer layer thickness of the coatings were measured at 10 points on each cross section using a filar eyepiece microscope. The coating thickness distributions of all the EAPA coated specimens were also measured using a nondestructive,

eddy-current tester. This thickness distribution agreed well with that metallographically determined. No nondestructive thickness measurements were made on the CoCrAlY coated specimens because the instrument did not operate satisfactorily on that coating system.

After the test, selected specimens were also sectioned through the maximum temperature zone (3.18 cm (1.25 in.) from the top end of the bar) to determine the degradation and to provide a microstructure for comparison with the X-ray data taken in the same location. Photomicrographs were taken of such areas at a point along the side of the bar.

Microhardness determinations of various zones in the polished cross sections on selected specimens, as-received and after maximum test time, were made using the Tukon Microhardness Tester. The 136⁰ Diamond Pyramid Hardness (DPH) indenter was used with a 50-gram load. The values presented are the average of four determinations in a zone.

Electron microprobe. - Selected CoCrAlY coated specimens were analyzed with the electron microprobe. Secondary electron backscatter images and X-ray fluorescence images for the elements, cobalt, chromium, aluminum, nickel, yttrium, molybdenum, tantalum, tungsten, and titanium were made. The probe was operated at 30 kilovolts and 50 nanoamperes with a 1-micrometer-diameter beam. Photographs were taken of the images on the display screen, which were at about $\times 200$ magnification.

RESULTS AND DISCUSSION

Embedded-Alumina-Particle-Aluminide (EAPA) Coatings

Coating characteristics. - X-ray diffraction of the as-coated surface revealed two phases: beta NiAl and alpha Al₂O₃ (table II). The designation "beta NiAl" refers to the type of phase; it can exist with a range of aluminum concentrations as well as with other elements substituted for nickel or aluminum. The X-ray fluorescence analysis of the as-coated surface revealed a noticeable increase in aluminum content compared with the substrate (table III) as would be expected. All of the other elements except nickel decreased in concentration relative to the bare alloy.

Photomicrographs of the as-deposited EAPA coatings on IN-100 and VIA are shown, respectively, in figures 3(a) and 4(a). On IN-100, the outer beta NiAl layer contains clumps of the 2-micrometer alumina (approx. 15 vol. %) (ref. 1) and has a hardness of 740 DPH. An inner layer of gamma prime plus beta NiAl can be seen with a few carbides in it. On VIA (fig. 4(a)) the outer beta NiAl layer has a hardness of only 460 DPH and the inner layer is multiphased showing that the same process does not deposit identi-

TABLE II. - X-RAY DIFFRACTION RESULTS OF AS-RECEIVED AND CYCLIC OXIDIZED
AT 1093° C (2000° F) AND MACH 1 EAPA COATED VIA AND IN-100 ALLOYS

Substrate alloy	Portion of coating studied	Exposure time, hr	Phase				
			β (NiAl) (lattice parameter, m; Å)	Gamma or gamma prime	α Al ₂ O ₃	TiO ₂	Spinel ^a
							NiAl ₂ O ₄ (lattice parameter, m; Å)
X-ray diffraction relative intensity ^b							
IN-100	Thick area	0	VS (2.88×10 ⁻¹⁰ ; 2.88)	--	S	---	-----
	Thick and thin areas	100	VS (2.88×10 ⁻¹⁰ ; 2.88)	--	S	---	-----
	Thick area	400	S (2.86×10 ⁻¹⁰ ; 2.86)	W	S	---	T (8.06×10 ⁻¹⁰ ; 8.06)
	Thin area	400	-----	VS	S	VW	VW (8.08×10 ⁻¹⁰ ; 8.08)
VIA	-----	0	VS (2.87×10 ⁻¹⁰ ; 2.87)	--	M	---	-----
	-----	100	M (2.86×10 ⁻¹⁰ ; 2.86)	S	S	W	W (8.08×10 ⁻¹⁰ ; 8.08)
	-----	400	VW (2.86×10 ⁻¹⁰ ; 2.86)	VS	S	---	W (8.12×10 ⁻¹⁰ ; 8.12)

^aLattice parameter for pure NiAl₂O₄ is 8.05×10⁻¹⁰ m (8.05 Å).

^bStrong, S; medium, M; weak, W; very weak, VW; trace, T.

TABLE III. - X-RAY FLUORESCENCE ANALYSIS RESULTS FOR EAPA COATED SPECIMENS

Substrate alloy	Exposure time, hr	Al	Cr	Co	Ti	Mo	V	Ni	Fe	Si	Nb	Hf	Ta	W
		Ratio of observed counts to that of standard ^a												
IN-100	b ₀	9.6	0.22	0.75	0.05	0.52	0.08	1.2	0.36	0.56	----	----	----	----
	100	25	.13	.78	1.2	.71	.54	.89	.51	.28	----	----	----	----
	400	14	.08	.56	.96	.68	.38	.67	1.1	5.2	----	----	----	----
VIA	b ₀	2.2	0.20	0.71	0.05	0.53	----	1.4	0.69	0.03	0.48	0.28	0.03	0.10
	100	5.2	.72	.92	.53	.48	----	1.1	.69	.26	.55	2.2	.63	.16
	400	4.6	1.0	1.0	.61	.85	----	1.0	.85	.67	.84	2.3	.68	.33

^aThe standard was bare IN-100 or VIA, whichever pertinent; an average of two specimens was used.

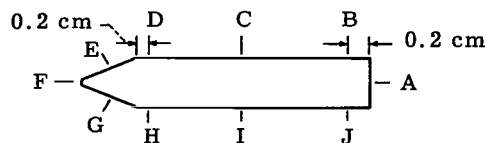
^bAverage of three specimens.

cal coatings on substrates of different chemistry. Again, however, the alumina is present in clumps in the beta NiAl outer layer.

Tables IV(a) and (b) show the variation of the coating thickness at intervals from the top to the bottom of the specimen and around the circumference at each interval as measured metallographically. On IN-100 the coating thickness ranged from thin spots of 0.001 centimeter to thicker areas of 0.0058 centimeter; on VIA the coating thickness distribution was more uniform, ranging from 0.0025 to 0.0062 centimeter with no very

TABLE IV. - COATING THICKNESS DISTRIBUTION FOR EAPA COATING AS RECEIVED

[Thickness determined metallographically.]



Substrate alloy	Distance of cross section from top end of bar		Position on cross section (see sketch)									
			A	B	C	D	E	F	G	H	I	J
	cm	in.	^a Coating thickness, cm									
IN-100	1.27	0.5	{ 0.0058	0.0050	0.0049	0.0040	0.0042	0.0053	0.0040	0.0040	0.0053	0.0055
			-----	-----	-----	-----	-----	-----	-----	-----	-----	-----
	2.54	1.0	{ .0041	.0046	.0040	.0026	.0035	.0040	.0030	.0028	.0048	.0050
			{ .0020	.0020	.0020	.0015	.0015	.0010	.0020	.0020	.0025	.0025
3.81	1.5	{ .0040	.0045	.0035	.0019	.0028	.0038	.0019	.0020	.0035	.0045	
		-----	-----	-----	-----	-----	-----	-----	-----	-----	-----	
5.08	2.0	{ .0045	.0046	.0036	.0018	.0032	.0037	.0026	.0025	.0036	.0048	
		{ .0025	.0025	.0020	.0010	.0020	.0015	.0010	.0010	.0020	.0025	
VIA	1.27	0.5	{ 0.0062	0.0053	0.0048	0.0042	0.0045	0.0048	0.0043	0.0042	0.0045	0.0055
			-----	-----	-----	-----	-----	-----	-----	-----	-----	-----
	2.54	1.0	{ .0060	.0045	.0045	.0042	.0042	.0040	.0045	.0045	.0042	.0048
			{ .0035	.0020	.0020	.0025	.0025	.0025	.0025	.0020	.0025	.0025
3.81	1.5	{ .0045	.0046	.0045	.0046	.0043	.0045	.0041	.0038	.0040	.0045	
		-----	-----	-----	-----	-----	-----	-----	-----	-----	-----	
5.08	2.0	{ .0038	.0045	.0042	.0042	.0040	.0040	.0045	.0042	.0046	.0042	
		{ .0025	.0025	.0020	.0025	.0025	.0020	.0025	.0025	.0025	.0025	.0025

^aTop value is total thickness of the coating; bottom value is the thickness of outer layer β (NiAl) of the coating.

thin areas.

Weight change and appearance. - The 1093^o C (2000^o F), high-velocity-gas, 1-hour cyclic oxidation weight change results for the EAPA coatings on IN-100 and VIA are presented in figures 5 and 6 along with similar data for other aluminide coatings and bare alloys. The time at which the first thermal fatigue crack was noticed for each system is also given on figure 5.

The EAPA coating afforded oxidation protection to IN-100 for about 120 to 150 hours (see fig. 5(a)); the fused-salt aluminide coating for about 240 hours; and the commercial coatings from 60 to 160 hours based on time to show a turn-around in the weight change curves. The bare IN-100 lost weight from the start of testing. Thermal fatigue cracks were observed after 40 hours on bare IN-100 and grew to almost 0.63 centimeter (0.25 in.) long after 100 hours (fig. 7(a)). Fatigue cracks first appeared after 120 hours

on EAPA coated IN-100 and were more than 0.63 centimeter long after 400 hours. The fused salt applied coating (ref. 4) showed no cracks up to 300 hours of testing - the total test time in that study. Considering that the EAPA coating is the thinnest of the coatings tested, it performed about as well as the two commercial pack aluminide coatings on IN-100, but not as well as the fused-salt aluminide coating. Whether it would have performed significantly better, due to the particle embedment, if tested at the same coating thickness, cannot be assessed.

Figure 5(b) shows the weight change results for the EAPA and other coatings on VIA. On the basis of time before weight loss occurs, the EAPA coating provided oxidation protection for about 60 to 70 hours; this is comparable to the two commercial aluminide coatings containing no embedded alumina particles even though the EAPA coating is somewhat thinner. The bare VIA lost weight from the start. Thermal fatigue cracks were detectable (fig. 7(d)) on the bare VIA at 40 hours and by 100 hours grew to about 0.63 centimeter (0.25 in.). There were no fatigue cracks in the EAPA coated VIA after 400 hours of testing, but a few surface oxide pits were present after 100 hours (figs. 7(e) and (f)). Neither commercial pack aluminide coating showed leading-edge cracks after 300 hours of testing, but one showed some trailing-edge cracks. Again, the EAPA coating performed quite similarly to the commercial coatings without the alumina additions.

While there was no difference in the tendency of bare IN-100 and VIA to crack, the EAPA and also commercial aluminide coatings on VIA showed a lesser tendency to crack than the IN-100 coated by the same processes. This is probably traceable to the lower initial hardness of the beta NiAl layer on the VIA (interpreted to mean greater ductility) and the nonuniform, thinner coating on IN-100, especially on leading edges.

In figure 6 burner rig test data for EAPA coated VIA are shown as obtained on different specimen geometries, bow paddle and NASA wedge, and under different gas velocities and cooling conditions. All data are for 1-hour cycles with a maximum exposure temperature of 1093^o C (2000^o F). For comparison, some data for an alumina plus titania particle enriched coating are also presented. This coating has been used in actual aircraft gas turbine engines. Both coatings have approximately the same total thickness.

The comparative coating data given in figure 6(c) for the highest gas velocity test is the average of the data for the two commercial pack aluminide coatings presented separately in figure 5(b). In rig 1 (ref. 1) at Mach 0.05 the EAPA coating is protective, based on the time to the change in the slope of the weight change curve for 500 to 600 hours; in rig 2 (ref. 1) at Mach 0.5 it was protective 100 to 150 hours; and in the Lewis high-gas-velocity tester, for only 60 to 100 hours.

Although there are differences in specimen geometry, burner fuel, flame pattern, coating thicknesses and etc., it appears that the protective life of the EAPA coating decreases as the Mach number (gas velocity) of the test rig and/or the severity of cooling

on each cycle increase. Furthermore, from an examination of figures 6(a) and (b), it is concluded that, on a weight change basis, the EAPA coating containing only alpha alumina particles affords longer protection in the lower velocity tests than the baseline coating containing both alumina and titania. However, this advantage decreases with the increasing severity of test, and, in the Lewis high-velocity-gas tests, the two coatings might be expected to perform about the same.

Posttest examination of specimens. - To provide information on the nature of the degradation of the EAPA coating on IN-100 and VIA tested at high gas velocity and 1093° C (2000° F), X-ray diffraction, X-ray fluorescence, and metallographic examinations of specimens were made after 100 and 400 hours. The results are presented in tables II and III and figures 3 and 4.

The X-ray diffraction results are summarized in table II. (The designation beta NiAl refers to the type of phase; it can exist with a range of aluminum concentrations as well as with other elements substituted for Ni or Al.) After 100 hours, the alpha alumina and beta NiAl phases alone were detected on IN-100 in both thick and thinly coated areas. However, after 400 hours of testing the thickly coated areas show, in addition, a trace of spinel and gamma+gamma prime phases. The more thinly coated areas show no beta NiAl after 400 hours but considerable amounts of gamma, gamma prime, alpha alumina, and very small amounts of titania and spinel. This spinel is believed to be mainly NiAl₂O₄. The X-ray diffraction results are very similar for the EAPA coated VIA in that there appears to be a decrease in beta NiAl and increases in gamma and gamma prime with increased exposure time.

The X-ray fluorescence results are presented in table III. The values given are ratios of the element counts in or near the surface to that of the bare alloy. These ratios only have usefulness for comparing the same element and cannot be used quantitatively. It appears that the aluminum, iron, vanadium, and titanium content of the surface of the EAPA coated IN-100 increased during the first 100 hours of cyclic oxidation, that the chromium, silicon, and nickel contents decreased and, that the cobalt remained about the same. From 100 to 400 hours the iron and silicon continued to increase, the aluminum, chromium, nickel, vanadium, titanium, and cobalt decreased, and the molybdenum remained essentially unchanged. The aluminum, titanium, chromium, silicon, hafnium, and tantalum content of the surface of the EAPA coated VIA increased in the first 100 hours, while molybdenum and nickel decreased. From 100 to 400 hours the aluminum decreased only slightly, and the rest of the elements either increased or remained the same as at 100 hours. On IN-100 the chromium decreased continuously, but on VIA it increased continuously.

The X-ray diffraction and fluorescence results taken together with visual observations and information contained in references 4 and 5 suggests that the major degradation of the EAPA coatings on both alloys can be attributed to the loss of aluminum -

mainly by oxide spalling. On IN-100, the substrate elements, particularly titanium, have entered the surface and are also affecting the oxidation performance in an as yet not well defined way.

Figures 3(b) and (c) and 4(b) and (c) present the microstructures of the EAPA coated IN-100 and the VIA after 100 and 400 hours of testing at 1093°C (2000°F). The phases and their distribution have been tentatively identified from X-ray diffraction, X-ray fluorescence, and by analogy to structures presented in references 4 to 6. The results in figure 3(b) for the EAPA coated IN-100 show that at 100 hours the thickness of the beta NiAl layer has not changed appreciably but that the total coating layer has increased in thickness because of coating-substrate interdiffusion. Beneath the beta NiAl layer, which contains the clumps of alumina, a layer of gamma prime and then a layer of gamma solid solution containing carbides can be seen. This sequence was arrived at by, among others, analogy with the observations in reference 4 where gamma was identified at the substrate-coating interface through its relatively high chromium content. One grain of the beta NiAl shows the martensitic striations typical of nickel rich beta NiAl (ref. 7), and is another indication of aluminum loss from the coating. After 400 hours (fig. 3(c)) the surface oxide of alumina is supported by a gamma layer, a gamma prime layer containing the alumina particles as well as some gamma, and then another gamma layer at the substrate interface. The coating has been completely degraded; no beta NiAl appears to be left, and the absence of beta NiAl is supported by the rapid weight loss, which can be observed in figure 5(a).

The microstructures of the EAPA coated VIA alloy are presented in figure 4. After 100 hours of testing, the coating has thickened as in the case of the coated IN-100, but here it appears that the beta NiAl layers have grown because of a continued outward diffusion of nickel. A thin layer of alumina on the surface covers the beta NiAl plus alumina particle layer, which contains islands of gamma prime. Then a gamma-gamma prime layer can be seen. Again, the striated martensitic beta NiAl grains are seen, but here they are large, which indicates that the alumina particles do not inhibit their growth. Both the gamma prime islands and the martensitic structure indicate that the beta NiAl has begun to lose aluminum and is degrading. By 100 hours the degradation of the beta NiAl layer has proceeded to the point that the weight change data indicate a turn-around toward weight losses (fig. 5(b)). After 400 hours the coating is in an advanced stage of degradation (fig. 4(c)), and the slope of the weight loss curve is highly negative. Some small amount of beta NiAl still appears to be left near the coating-substrate interface on VIA as opposed to none on IN-100. This may be explained by either the thicker beta or different chemistry of VIA than IN-100. The refractory metals in the VIA substrate may be acting as a diffusion barrier and inhibiting substrate element dilution of the coating.

The microstructures reaffirm the fact that the degradation of the EAPA coating on both alloys is due to loss of aluminum from the beta NiAl layer. This loss does not appear to be inhibited by the presence of alumina particles. Thus these coatings degrade similarly to commercial aluminide systems. The substrate chemistry appears to influence both the initial microstructure of the aluminide coatings, the extent and nature of the elements which diffuse outward toward the surface, and the thermal crack resistance.

Cobalt-Chromium-Aluminum-Yttrium Coatings

Coating characteristics. - The overlay CoCrAlY coatings are nominally Co-22Cr-14Al-0.1Y (ref. 2). X-ray diffraction analysis of the as-coated surface (table V) revealed beta CoAl and cobalt solid solution as the only phases present in the coating on IN-100. The coating on alloy VIA, in addition, showed a trace of yttrium oxide (Y_2O_3). As expected, because this is an overlay and not a complete diffusion coating, the X-ray fluorescence results (table VI) show a pronounced increase in the concentration of the coating elements with respect to the substrate alloy and a sharp decrease in substrate elements. The very large ratio for yttrium reflects the fact that the substrate alloys have essentially no yttrium in them.

Photomicrographs of the as-coated alloys are presented in figure 8. The outer layers contain thin, columnar grains of cobalt solid solution and beta CoAl with a thin diffusion zone at the substrate interface. Based on subsequent microprobe analysis and the metallography (ref. 2) of oxidized specimens, the dark phase is believed to be the beta CoAl phase. The hardness of these coatings (570 DPH on IN-100, 680 DPH on VIA) is intermediate between the previously discussed aluminide hardnesses on the two alloys. Here the CoCrAlY coating on VIA appears harder than that on IN-100; the reverse was true for the aluminide coatings.

The longitudinal and vertical distribution of the coating thickness on both substrates is presented in table VII. The thickness measurements were performed in the same manner as those for the EAPA coatings. The results indicate a thickness variation of about 0.002 to 0.004 centimeter from side to side and about 0.001 to 0.002 centimeter from top to bottom. The coating thickness on VIA ranged from 0.011 to 0.015 centimeter, and on IN-100 it was 0.016 to 0.022 centimeter. The thicknesses of these coatings are greater than the EAPA coatings. The EAPA coating on VIA ranged from 0.0038 to 0.006 centimeter thick and on IN-100 from 0.001 to 0.0058 centimeter.

Oxidation weight change and appearance. - The high-gas-velocity tests ($1093^{\circ}C$ ($2000^{\circ}F$), 1-hr cycles) produced weight changes for the CoCrAlY coated IN-100 and VIA as shown in figure 9. For comparative purposes, the previously presented alumi-

TABLE V. - X-RAY DIFFRACTION RESULTS FOR AS-RECEIVED AND CYCLIC OXIDIZED CoCrAlY COATED VIA AND IN-100 ALLOYS

Substrate alloy	Exposure time, hr	Phase						
		$\beta(\text{CoAl})$ (lattice parameter, m; Å)	Co (solid solution) lattice parameter, m; Å	Y_2O_3	$\text{Y}_4\text{Al}_2\text{O}_9$	$\alpha\text{Al}_2\text{O}_3$	Co_3O_4	Spinel ^a
		CoCr ₂ O ₄ (lattice parameter, m; Å)						
X-ray diffraction relative intensity ^b								
IN-100	0	VS (2.86×10^{-10} ; 2.86)	S (3.57×10^{-10} ; 3.57)	--	--	--	---	-----
	100	T (2.86×10^{-10} ; 2.86)	S (3.57×10^{-10} ; 3.57)	--	--	S	---	-----
	300	-----	S (3.58×10^{-10} ; 3.58)	--	--	S	S	VW (8.28×10^{-10} ; 8.28)
VIA	0	VS (2.86×10^{-10} ; 2.86)	S (3.56×10^{-10} ; 3.56)	T	--	--	---	-----
	100	-----	S (3.57×10^{-10} ; 3.57)	--	--	S	---	-----
	600	-----	S (3.58×10^{-10} ; 3.58)	--	W	S	VW	VW (8.28×10^{-10} ; 8.28)

^aLattice parameter of CoCr₂O₄, 8.32×10^{-10} m (8.32 Å).

^bVery strong, VS; strong, S; weak, W; very weak, VW; trace, T.

TABLE VI. - X-RAY FLUORESCENCE ANALYSIS RESULTS FOR CoCrAlY COATED SPECIMENS

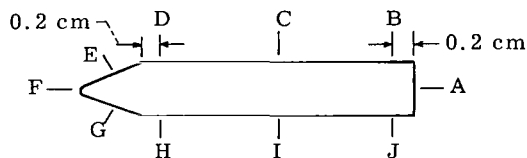
Substrate alloy	Exposure time, hr	Al	Cr	Co	Ti	Mo	V	Ni	Fe	Si	Y	Nb	Hf	Ta	W
		Ratio of observed counts to that of standard ^a													
IN-100	0	2.4	3.3	3.9	0.005	0.005	0	0.004	0.24	0.40	191 ^b	----	----	----	----
	100	27	2.0	2.2	.16	.46	.24	.27	.29	2.9	423	----	----	----	----
	300	16	1.2	1.5	.89	.61	.23	.30	.30	7.7	377	----	----	----	----
VIA	0	1.3	5.4	8.1	0.009	0.002	----	0.004	0.49	0.21	135	0.06	0	0.008	0
	100	5.7	3.3	4.8	.11	.54	----	.29	.60	.81	288	.51	1.0	.21	.09
	600	3.8	1.2	2.6	.16	.82	----	.38	.94	6.3	177	.50	2.8	.45	.20

^aThe standard was bare IN-100 or VIA, whichever pertinent; an average of two specimens was used.

^bSince the bare alloys contained little Y these values are artificially large.

TABLE VII. - COATING THICKNESS DISTRIBUTION OF CoCrAlY COATED ALLOYS (AS RECEIVED)

[Thickness determined metallographically.]



Substrate alloy	Distance of cross section from top end of bar		Position on cross section (see sketch)									
			A	B	C	D	E	F	G	H	I	J
	cm	in.	^a Coating thickness, cm									
IN-100	1.27	0.5	{ 0.0185	0.0182	0.0180	0.0175	0.0178	0.0195	0.0215	0.0215	0.0210	0.0205
			{ -----	-----	-----	-----	-----	-----	-----	-----	-----	-----
	2.54	1.0	{ .0180	.0188	.0185	.0185	.0180	.0210	.0215	.0216	.0210	.0205
			{ .0155	.0165	.0165	.0165	.0160	.0185	.0190	.0190	.0185	.0170
3.81	1.5	{ .0196	.0193	.0187	.0187	.0190	.0212	.0218	.0222	.0220	.0215	
		{ -----	-----	-----	-----	-----	-----	-----	-----	-----	-----	
5.08	2.0	{ .0205	.0195	.0191	.0188	.0186	.0212	.0225	.0220	.0212	.0212	
		{ .0180	.0175	.0170	.0165	.0165	.0185	.0200	.0195	.0185	.0185	
VIA	1.27	0.5	{ 0.0150	0.0155	0.0155	0.0150	0.0145	0.0140	0.0130	0.0132	0.0127	0.0125
			{ -----	-----	-----	-----	-----	-----	-----	-----	-----	-----
	2.54	1.0	{ .0155	.0162	.0155	.0155	.0145	.0145	.0135	.0132	.0132	.0127
			{ .0110	.0150	.0140	.0140	.0130	.0130	.0125	.0125	.0125	.0115
3.81	1.5	{ .0155	.0165	.0162	.0152	.0152	.0145	.0129	.0128	.0130	.0128	
		{ -----	-----	-----	-----	-----	-----	-----	-----	-----	-----	
5.08	2.0	{ .0155	.0155	.0152	.0148	.0152	.0150	.0135	.0129	.0130	.0128	
		{ .0140	.0140	.0142	.0136	.0142	.0140	.0120	.0115	.0115	.0115	

^aTop value is total thickness of the coating; bottom value is thickness of outer layer of the coating.

nide test data are also given in this figure. Figure 9(a) shows the results of these coatings on IN-100. It is apparent from the curves that CoCrAlY behaves similarly to the aluminide coatings even though it is considerably thicker. However, the coating did not crack in 300 hours of testing even though some oxide pits developed as shown in figure 10. In contrast, both aluminide coatings cracked before 300 hours.

The weight change results for similarly tested CoCrAlY coated VIA are presented in figure 9(b). In addition to the aluminide test data, this figure contains the Mach 0.3 test data for CoCrAlY coated VIA bow paddles tested in jet fueled burner rigs (ref. 2). From the time to show a turn-around in weight change, the CoCrAlY tested in the high velocity gas afforded protection for about 450 hours; the aluminide coating for only 50 to 100 hours. Although some of this difference might be due to the increased thickness, it appears that, compared with the same coating on IN-100, which was even thicker, coating-substrate compatibility is an important factor. Also, no thermal fatigue cracks were observed on the CoCrAlY tested VIA (fig. 9(b)), but some pitting was observed at 600 hours (fig. 10(d)). In the Mach 0.3 tests there was no weight change turn-around in 1100 hours and no cracking. Based on crack resistance and weight change behavior, the CoCrAlY coating on VIA is significantly superior to the aluminide coatings. But this coating, of the composition used, does appear to be somewhat sensitive to substrate composition as noted by its poor performance on IN-100.

Posttest examinations. - In an attempt to characterize the degradation of the CoCrAlY coating on IN-100 and VIA alloys, selected specimens were examined by X-ray fluorescence, X-ray diffraction, metallography, and electron microprobe analysis after oxidation. The diffraction results are presented in table V; the fluorescence results in table VI; the microprobe images in figures 11 and 12; and the microstructures in figures 13 to 15.

X-ray diffraction (table V) showed that before cyclic oxidation the CoCrAlY coating surface on IN-100 contained beta CoAl, Co solid solution, and on VIA an additional trace of Y_2O_3 . After 100 hours both alloys showed the surface alumina scale and a disappearance of the beta CoAl phase. After 300 hours the surface scale on coated IN-100 exhibited additional Co_3O_4 and $CoCr_2O_4$ oxide phases. After 600 hours the coated VIA showed all the phases previously described and in addition some $Y_4Al_2O_9$. Thus, basically the beta CoAl phase was lost near the surface and oxides appeared in addition to alumina.

X-ray fluorescence data (table VI) show that the as-coated surfaces are higher in the coating elements than the uncoated alloys as would be expected. (The absolute results for Co, Cr, Al, and Y were very similar on both as-coated substrates.) After 100 hours aluminum and yttrium increase while chromium and cobalt decrease on both alloys. At 300 hours for IN-100 and at 600 hours for the VIA, the coating elements decreased with respect to the 100 hour values, and the substrate elements, especially ti-

tanium and silicon for IN-100 and silicon for VIA, increased noticeably.

In general, then, aluminum, chromium, and cobalt depletion and/or dilution of the CoCrAlY coating by the respective major substrate elements constitutes the degradation scheme for these alloys. The presence of the Co_3O_4 in the surface scale has been shown to produce increased spalling (ref. 8). Its increased presence on IN-100 may be the reason for or an indication of the less protective nature of the CoCrAlY on that alloy. Also, the presence of the $\text{Y}_4\text{Al}_2\text{O}_9$ on VIA may reflect or cause better oxidation resistance.

Electron microprobe X-ray raster images for cobalt, chromium, aluminum, yttrium, nickel, titanium, molybdenum, tantalum, and tungsten were obtained on cross sections of the CoCrAlY coated IN-100 after 300 hours of testing and on VIA after 600 hours of testing. The data are presented in figures 11 and 12, respectively. These figures also include optical photomicrographs and electron backscatter images of the areas analyzed. After 300 hours of cyclic oxidation, the surface of the coated IN-100 exhibits an intense white band in the aluminum raster scan, which indicates a high concentration of aluminum in this case caused by the Al_2O_3 surface scale. Beneath the scale, the cobalt, chromium, and aluminum images are all rather bright, identifying the aluminum rich cobalt-chromium solid solution. Farther from the surface, scattered islands appear. In this region, the cobalt image remains bright and the island areas appear to be brighter in the aluminum image, reflecting beta CoAl islands in a cobalt solid solution matrix. This same band contains smaller particles which etch differently and give bright titanium and molybdenum images, indicating carbides which were originally present in the substrate. Nickel appears to be contained in both the beta CoAl and the cobalt solid solution. Tantalum, yttrium, and tungsten were not found to any extent in the coating. The same general conclusions can be arrived at for the VIA alloy after 600 hours by examining the images in figure 12. The major difference is that the carbides in VIA are rich in titanium and tantalum. Also, the nickel image appears less bright, which indicates less dilution of the coating by nickel. This could be another reason for the greater oxidation resistance of the CoCrAlY coating on VIA than on IN-100.

The microstructure of the coatings after 100 hours on both alloys and after 300 and 600 hours on IN-100 and VIA, respectively, are shown in figures 13 and 14. After 100 hours of testing, a thin white layer of cobalt solid solution formed beneath the thin alumina surface scale on both alloys. The area beneath this region was feathery and acicular, especially on IN-100 (fig. 13(a)). This is the beta CoAl + Co(ss) region. Beneath the original coating, islands of beta CoAl can be seen in a cobalt solid solution matrix which also contains some carbides. After 300 hours of testing (fig. 13(b)) the coating on IN-100 has lost almost all of its acicular beta CoAl, and the diffusion zone containing the blocky beta CoAl and carbides appears to have grown. There are pronounced local oxide penetrations at the surface. After 600 hours of testing the coating on VIA (fig.



14(b)) has changed similarly except there is more acicular beta CoAl left and the zone beneath the original coating has not grown nearly as large even in twice the exposure time. In figures 13(c) and 14(c) both specimens were heavily etched to bring out the structure of the cobalt solid solution region. Note that on IN-100 this region has rather large grains and is twinned, while on VIA it has a much finer grain size. This is again a reflection of the CoCrAlY diffusional stability on the VIA substrate compared with IN-100. Figure 15 is the cross section of one of the deep, localized oxidation pits that have been observed in the CoCrAlY coating. Such pits provide a shorter path for environmental attack of the substrate and perhaps also sites for eventual thermal fatigue cracking.

In general, the degradation of the CoCrAlY coatings on both IN-100 and VIA also appears related to the loss of aluminum and the decomposition of the beta CoAl phase. The formation of an aluminum rich, cobalt-chromium solid solution offers continued protection and a relatively low hardness, which may be the prime factors in resistance of thermal fatigue. In the case of VIA, the high refractory metal content appears to minimize the coating-substrate interdiffusion and thus minimize the harmful dilution of the protective coating. The scale formed on CoCrAlY coated VIA also appears to have a lesser tendency to form the spall prone Co_3O_4 oxide.

CONCLUSIONS

The behavior of embedded alumina particle aluminized coatings (about 0.004 to 0.006 cm thick, i. e., in the same thickness range as commercial aluminide coatings) and CoCrAlY coatings (about 0.013 to 0.022 cm thick) on the nickel alloys IN-100 and TRW-NASA-VIA was studied in high-gas-velocity (approximately Mach 1) tests for 300 to 600 hours at 1093°C (2000°F) using 1-hour exposure cycles followed by air blast quenching. Based on weight change, visual, metallographic, and analytical results, the following conclusions may be drawn from this study:

1. The CoCrAlY coating on VIA provided the most oxidation resistant system tested and offered thermal fatigue crack protection of at least 600 hours. This is superior to the commercial and experimental aluminide coatings tested in this program and to most aluminide coatings previously examined at this laboratory. Although the CoCrAlY coating was thicker than the aluminide coatings tested, it was in the range of thicknesses that are feasible and are being considered for commercial engine usage.

2. The CoCrAlY coatings on both alloys showed no tendency toward thermal fatigue cracking in this test, which involves rapid quenching. This ability appears related to their good oxidation resistance and ductility as reflected by their relatively low hardness

(especially after CoAl is lost from very near the surface) compared with commercial aluminide coatings.

3. On IN-100 and VIA substrates, the alumina particle containing aluminide coatings performed similarly to commercial aluminide coatings containing no alumina particles.

4. Both embedded alumina particle aluminide (EAPA) and commercial aluminide coatings prevent thermal fatigue cracking in VIA alloy up to times of at least 300 to 400 hours. For both coating types on IN-100, cracks are present at 100 to 150 hours. This indicates a substrate influence on crack prevention by these coatings.

Lewis Research Center,
National Aeronautics and Space Administration,
Cleveland, Ohio, April 3, 1972,
134-03.

REFERENCES

1. Levinstein, M. A.; Stanley, J. R.: Improved Aluminide Coatings for Nickel-Base Alloys, General Electric Co. (NASA-CR-72863), Mar. 12, 1971.
2. Talboom, F. P.; Elam, R. C.; and Wilson, L. W.: Evaluation of Advanced Superalloy Protection Systems. Rep. PWA-4055, Pratt & Whitney Aircraft (NASA CR-72813), Dec. 2, 1970.
3. Johnston, James R.; and Ashbrook, Richard L.: Oxidation and Thermal Fatigue Cracking of Nickel- and Cobalt-Base Alloys in a High Velocity Gas Stream. NASA TN D-5376, 1969.
4. Sanders, William A.; Barrett, Charles A.; and Probst, Hubert B.: Evaluation of High-Gas-Velocity and Static Oxidation Behavior of Fused-Salt-Aluminided IN 100 Between 1038^o and 1149^o C. NASA TN D-6400, 1971.
5. Goward, G. W.; Boone, D. H.; and Giggins, C. S.: Formation and Degradation Mechanisms of Aluminide Coatings on Nickel-Base Superalloys. ASM Trans. Quart., vol. 60, no. 2, June 1967, pp. 228-241.
6. Smialek, James L.: Exploratory Study of Oxidation-Resistant Aluminized Slurry Coatings for IN 100 and WI-52 Superalloys. NASA TN D-6329, 1971.
7. Smialek, James L.: Martensite in NiAl Oxidation-Resistant Coatings. Metallurg. Trans., vol. 2, no. 3, Mar. 1971, pp. 913-915.
8. Lowell, Carl E.; and Drell, Isadore L.: Effect of Surface Preparation on Oxidation of WI-52 at 1800^o and 2000^o F (1255 and 1366^o K). NASA TN D-6148, 1971.

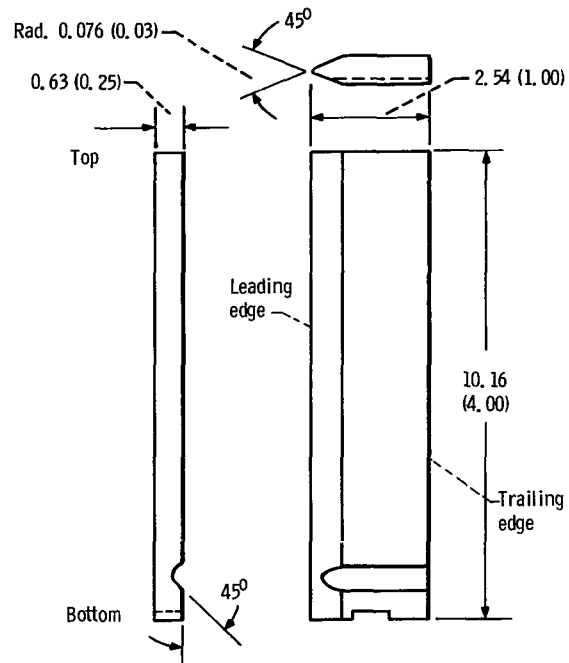
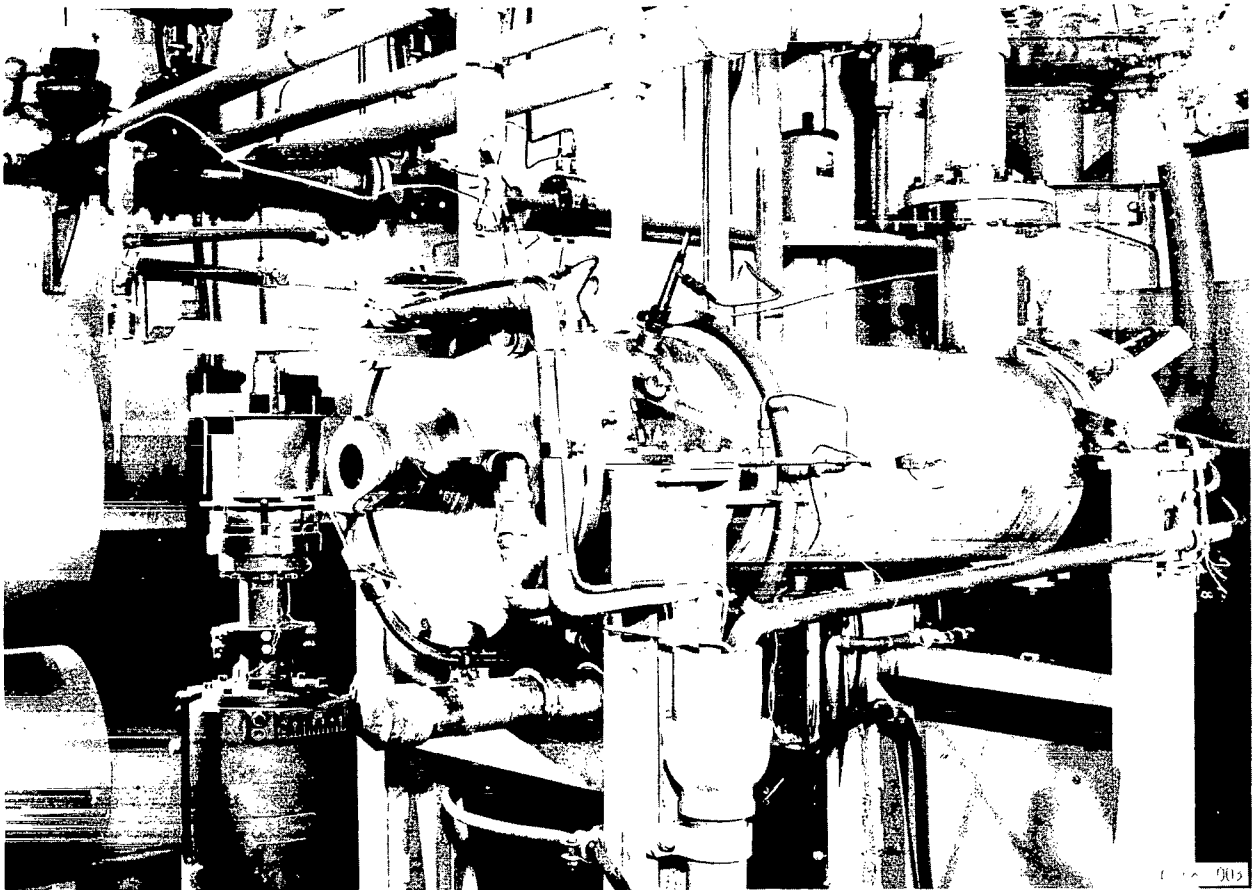
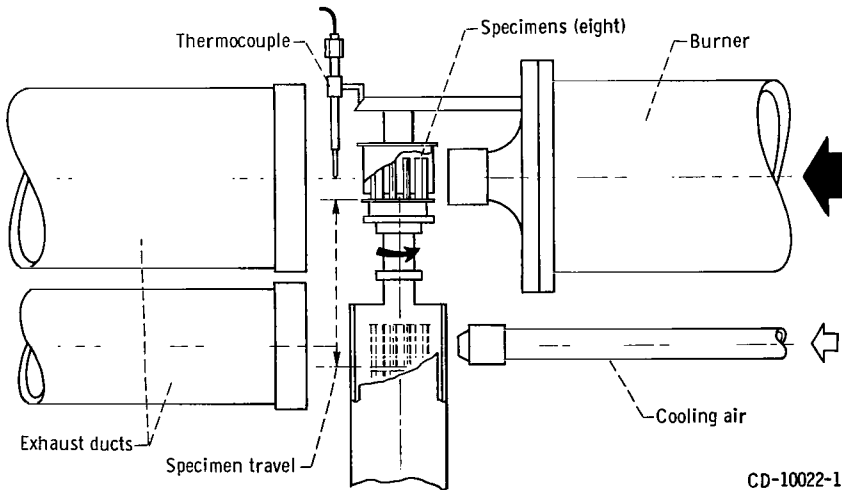


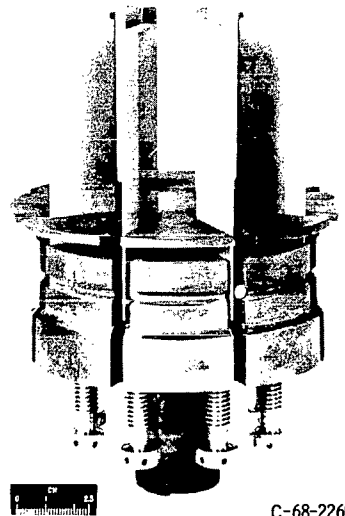
Figure 1. - Lewis wedge bar test specimen. (Dimensions are in cm (in.))



(a) Overall view.

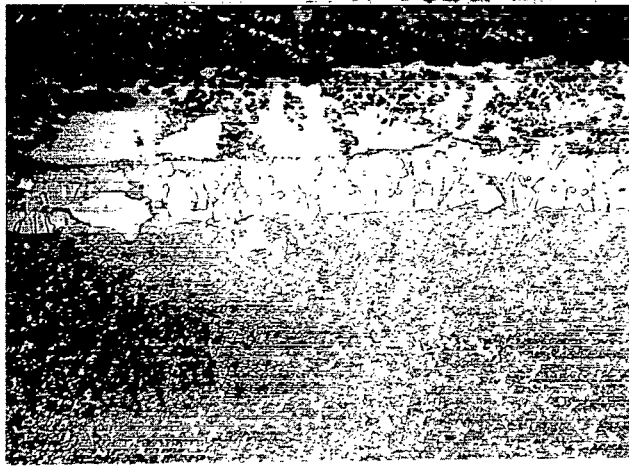


(b) Schematic diagram.



(c) Specimen holder assembly.

Figure 2. - High-gas-velocity oxidation apparatus.



β(NiAl), Al₂O₃
particles; 740 DPH

γ', β(NiAl), 800 DPH

γ, γ' substrate;
390 DPH

(a) As received.



αAl₂O₃ surface layer

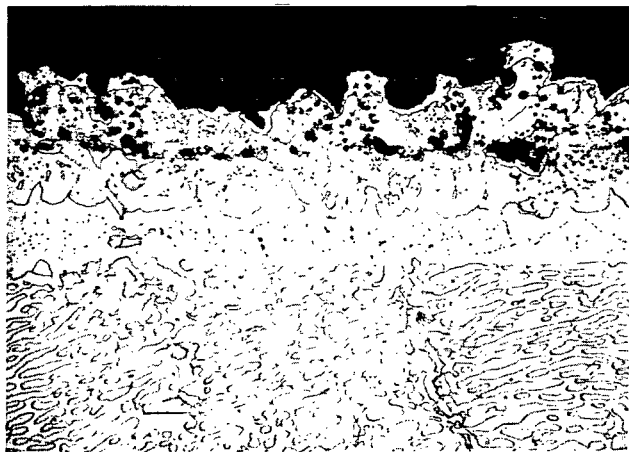
β(NiAl), αAl₂O₃
particles

γ'

γ

γ, γ'
substrate

(b) Cyclic oxidation, 100 hours.



αAl₂O₃ surface layer

γ

450 DPH

γ', αAl₂O₃ particles

340 DPH

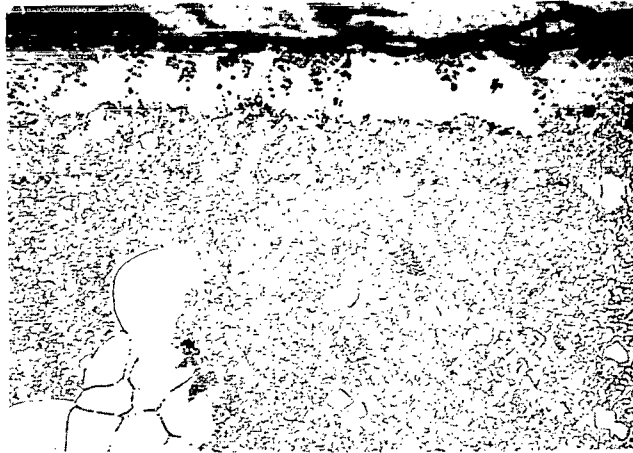
γ, 390 DPH

γ, γ' substrate;
410 DPH

0.0025 cm

(c) Cyclic oxidation, 400 hours.

Figure 3. - Microstructures of EAPA coated IN-100 after cyclic oxidation at 1093° C (2000° F) in high-velocity gas. (DPH denotes diamond pyramid hardness.)



$\beta(\text{NiAl})$, $\alpha\text{Al}_2\text{O}_3$
particles; 460 DPH

γ , γ' , $\beta(\text{NiAl})$, carbide rich
diffusion zone, 910 DPH

γ , γ' substrate;
495 DPH

(a) As received.



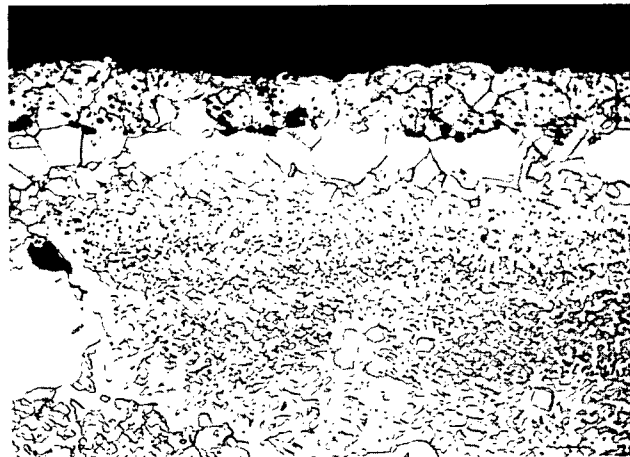
$\alpha\text{Al}_2\text{O}_3$ surface layer

γ' grain

γ' , $\beta(\text{NiAl})$

γ , γ' substrate

(b) Cyclic oxidation, 100 hours.



$\alpha\text{Al}_2\text{O}_3$ surface layer

----- 495 DPH
 γ' , $\alpha\text{Al}_2\text{O}_3$ particles

----- 410 DPH

 γ , γ' $\beta(\text{NiAl})$; 510 DPH

γ , γ' substrate;
480 DPH

0,0025 cm

(c) Cyclic oxidation, 400 hours.

Figure 4. - Microstructures of EPA coated VIA alloy after cyclic oxidation at 1093° C (2000° F) in high-velocity gas. (DPH denotes diamond pyramid hardness.)

Type of coating	Total coating thickness, cm	Thickness of outer NiAl layer, cm	Source of data
○ None	0	0	This study
△ None	0	0	Ref. 4
□ None	0	0	Ref. 3
□ EAPA	0.002-0.006	0.001-0.003	This study
◇ Fused salt, aluminized	.01	.006	Ref. 3
△ Commercial pack aluminide - no particle embedment	.013	.007	Unpublished data of author
▽ Commercial pack aluminide - no particle embedment	.007	.005	Unpublished data of M. A. Gedwill of Lewis

Type of coating	Total coating thickness, cm	Thickness of outer layer, cm	Source of data
○ None	0	0	This study
△ EAPA	0.004-0.006	0.002-0.004	This study
□ Commercial pack aluminide - no particle embedment	.011	.005	Unpublished data of author
△ Commercial pack aluminide - no particle embedment	.006	.004	Unpublished data of M. A. Gedwill of Lewis

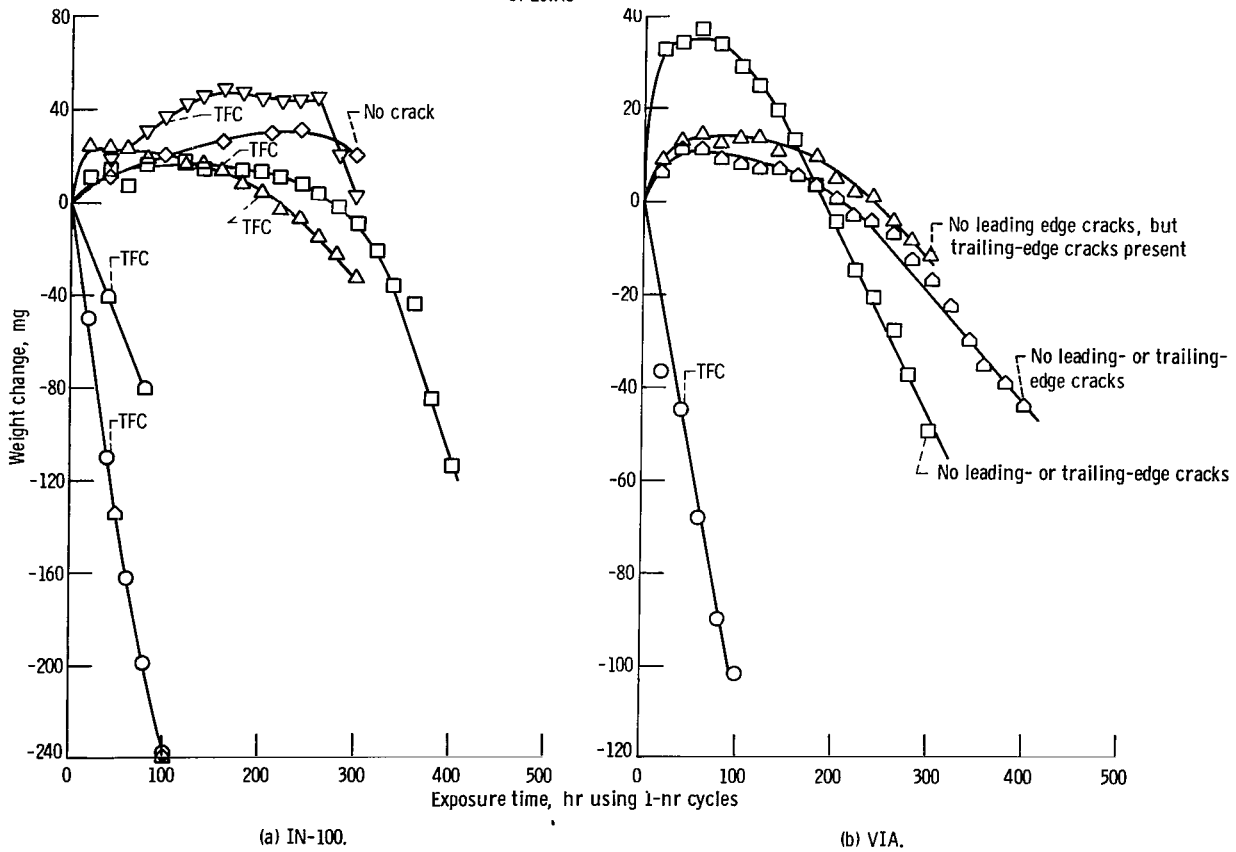
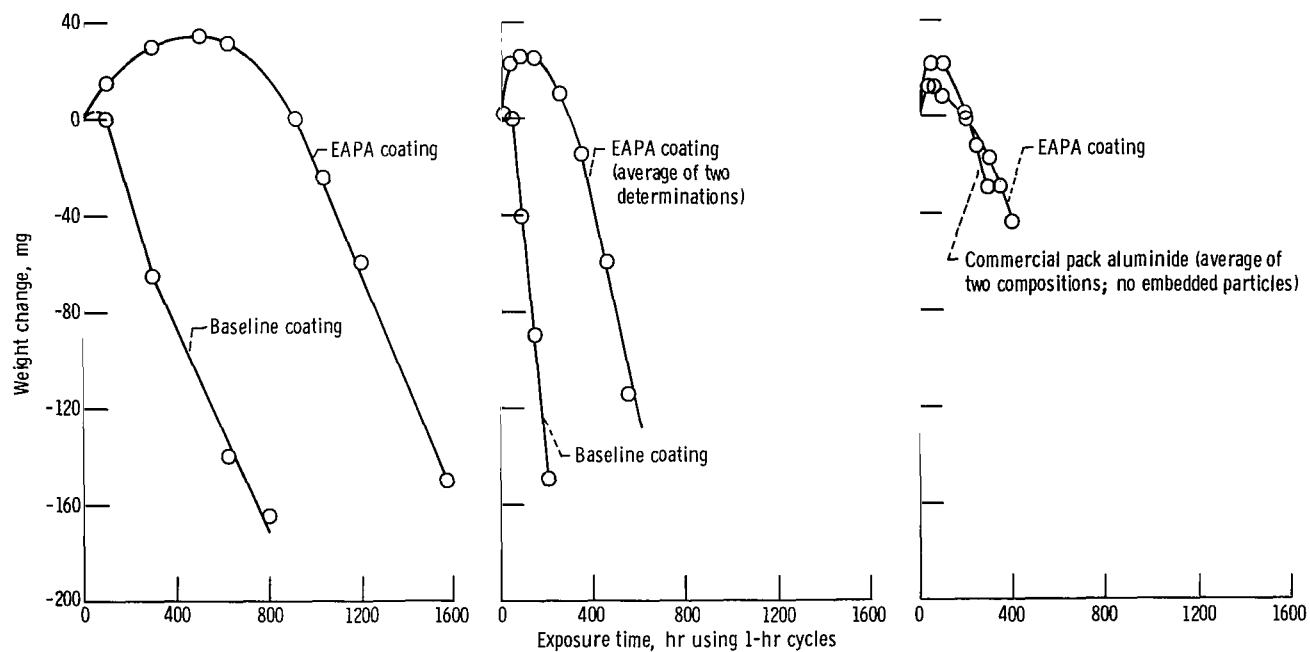


Figure 5. - High-gas-velocity cyclic oxidation weight-changes of coated and bare IN-100 and VIA at 1093° C (2000° F). All specimens were Lewis wedge bars. Note: TFC indicates that a thermal fatigue crack was observed.

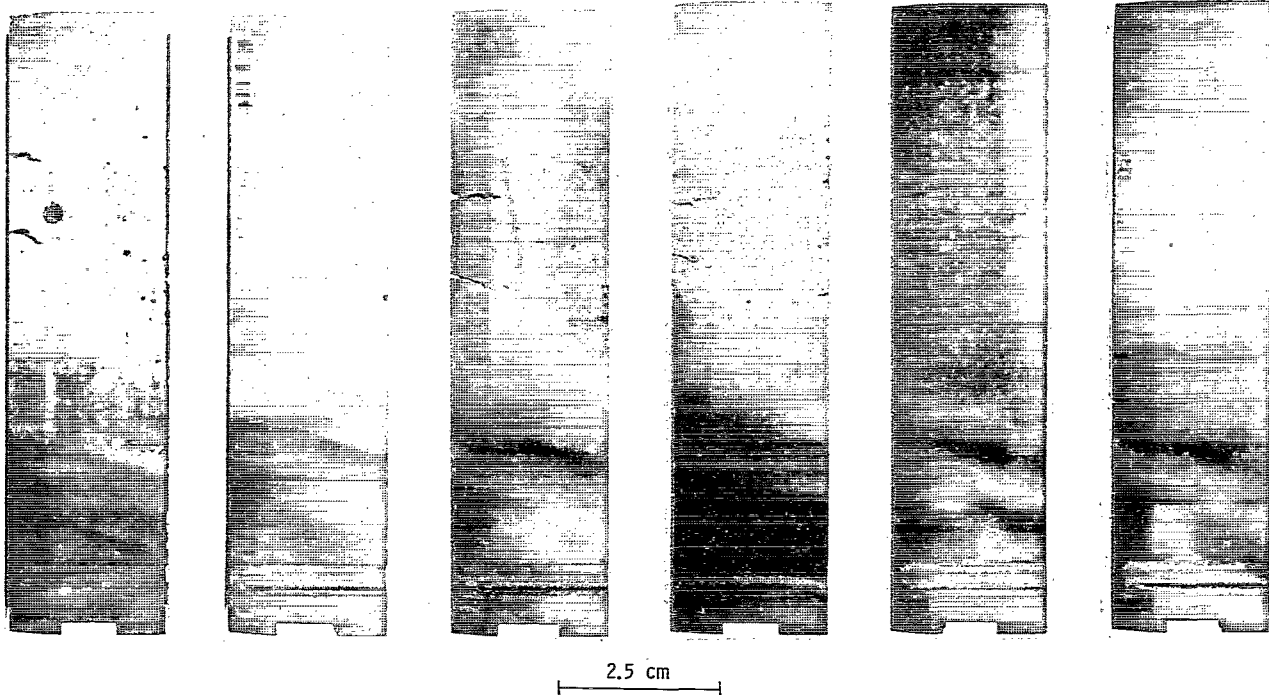


(a) Burner rig 1 (ref. 1). Mach 0.05; specimen rotation, 36 rpm; specimen geometry, paddles; cooling, 3-minute air blast to 482° C (900° F); fuel, natural gas; specimen area heated, approximately 40 square centimeters.

(b) Burner rig 2 (ref. 1). Mach 0.5; specimen rotation, 1750 rpm; specimen geometry, paddles; cooling, not given; fuel, type A jet fuel; specimen area heated, approximately 40 square centimeters.

(c) Lewis burner rig (this study). High gas velocity; specimen rotation, 900 rpm; specimen geometry, Lewis wedge bars; cooling, 3-minute blast to room temperature; fuel, natural gas; specimen area heated, approximately 30 square centimeters.

Figure 6. - Comparison of weight change of EAPA coated VIA with commercial pack aluminide coatings and baseline coatings ($\text{Al}_2\text{O}_3 + \text{TiO}_2$ particles embedded in aluminide coating) on VIA. Cyclic oxidation at 1093° C (2000° F).



(a) Bare IN-100; exposure time, 100 hours.

(b) EAPA coated IN-100; exposure time, 100 hours.

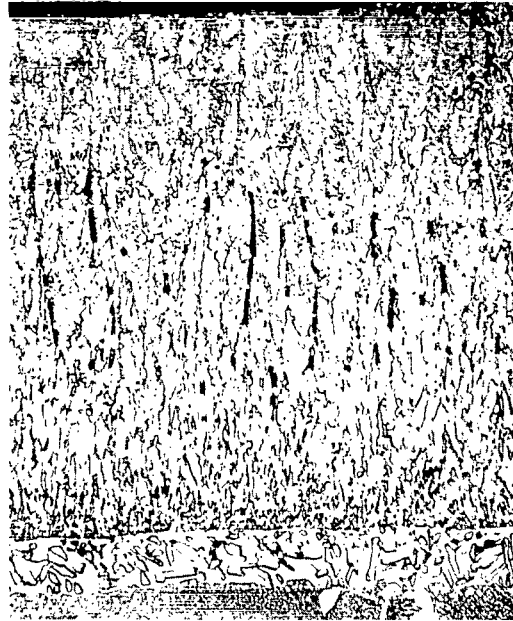
(c) EAPA coated IN-100; exposure time, 400 hours.

(d) Bare VIA; exposure time, 100 hours.

(e) EAPA coated VIA; exposure time, 100 hours.

(f) EAPA coated VIA; exposure time, 400 hours.

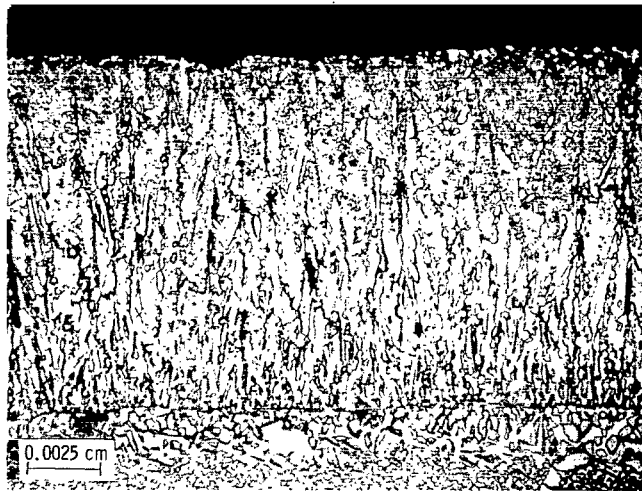
Figure 7. - Bare and EAPA coated IN-100 and VIA specimens after high-gas-velocity cyclic oxidation at 1093° C (2000° F) using 1 hour cycles.



β (CoAl),
Co(ss);
570 DPH

Diffusion
zone; 430 DPH
Substrate;
375 DPH

(a) IN-100 substrate.

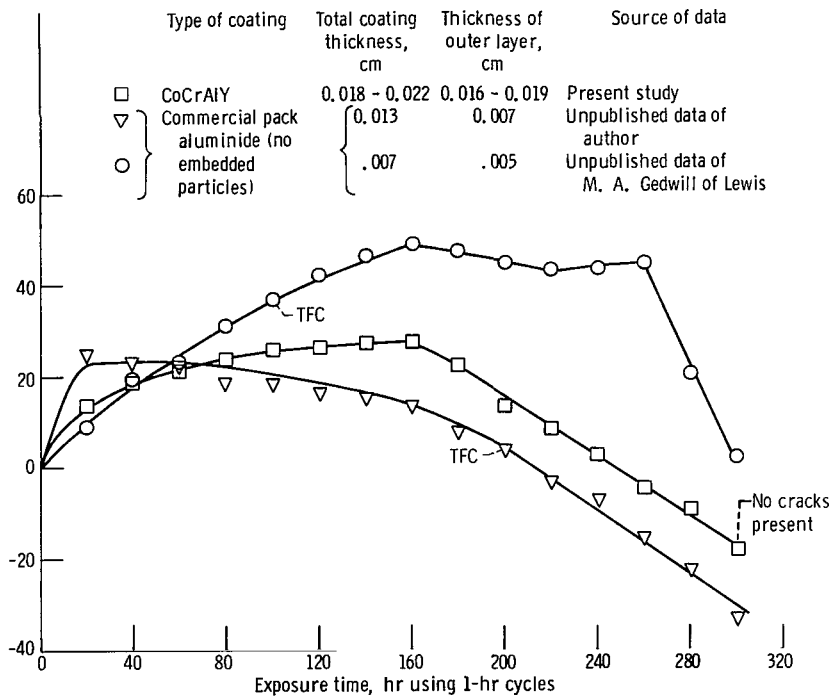


β (CoAl),
Co(ss);
680 DPH

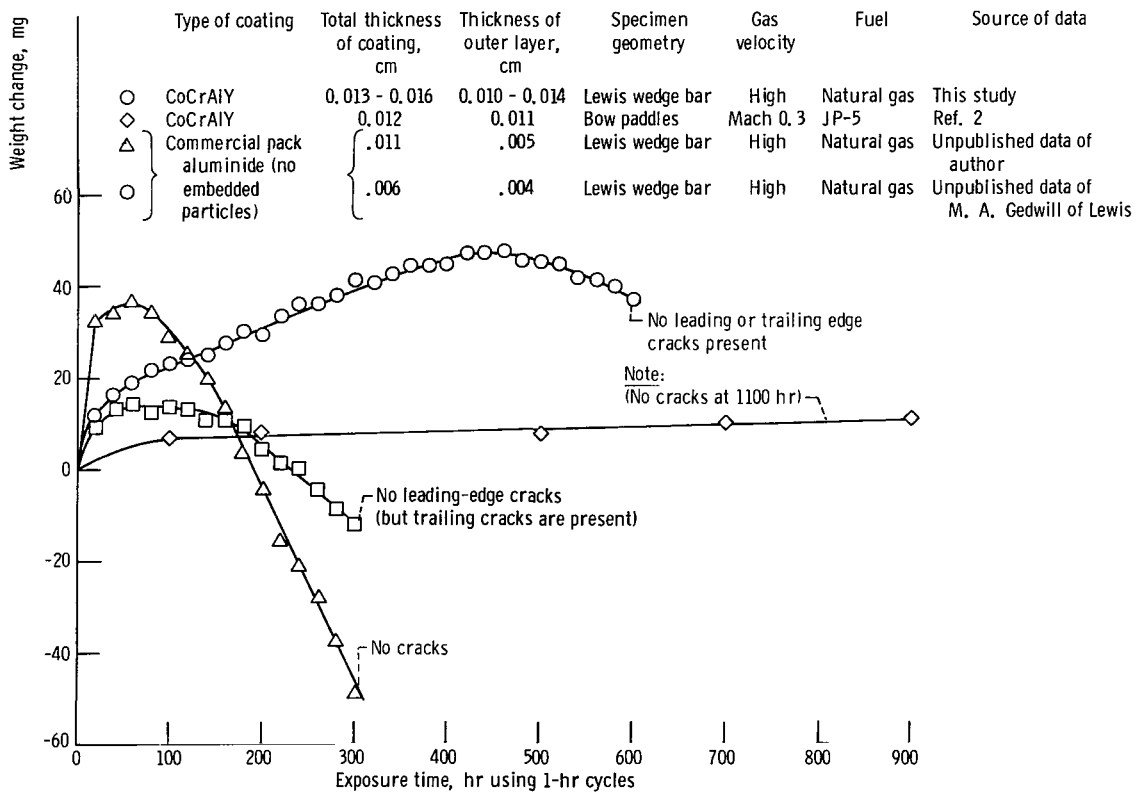
Diffusion
zone; 550 DPH
Substrate;
540 DPH

(b) VIA substrate.

Figure 8. - Microstructures of as-received CoCrAlY coated specimens. (DPH denotes diamond pyramid hardness.)

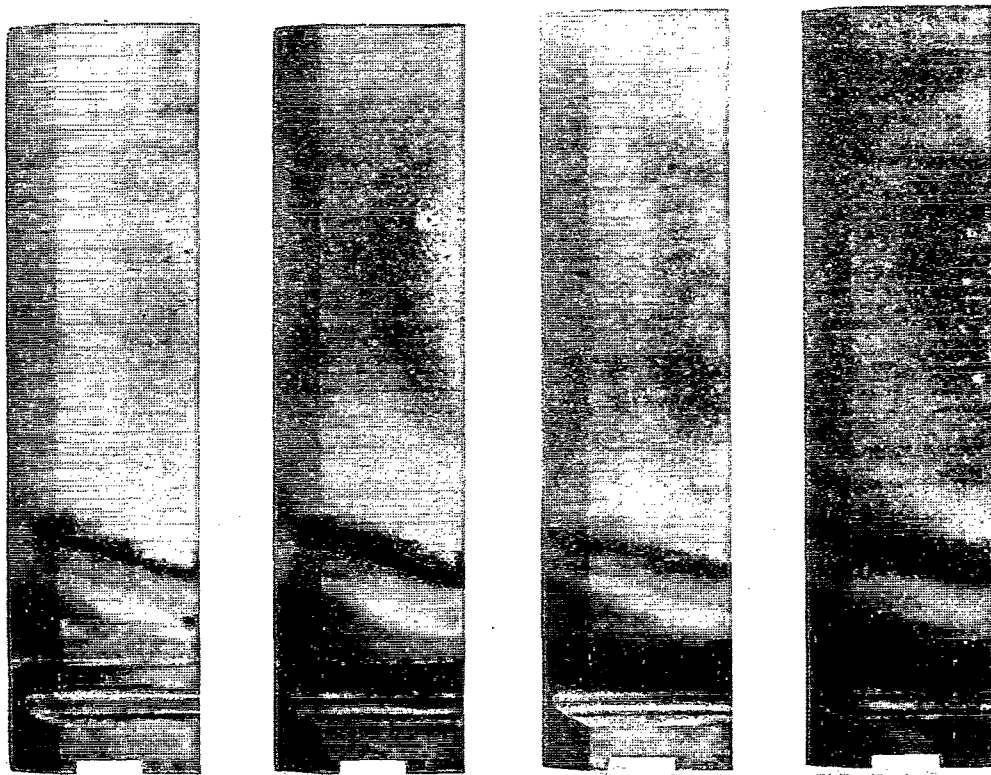


(a) Coated IN-100. High-gas-velocity data; specimen geometry, Lewis wedge bar.



(b) Coated VIA. High- and low-gas-velocity data; all specimens cooled 3 minutes to room temperature.

Figure 9. - Cyclic oxidation weight change of CoCrAlY coated IN-100 and VIA at 1093° C (2000° F). (TFC indicates that a thermal fatigue crack was observed.)



2.5 cm

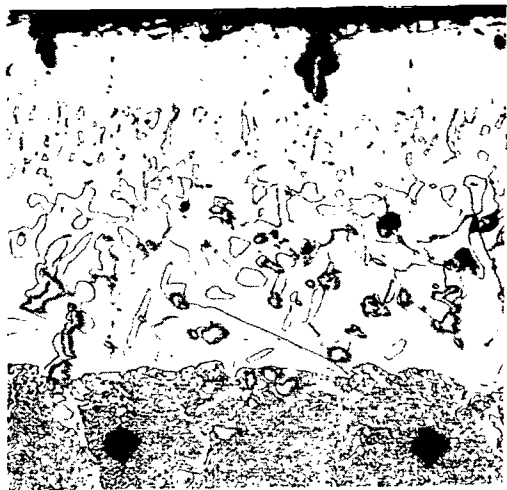
(a) CoCrAlY coated IN-100;
exposure time, 180
hours.

(b) CoCrAlY coated IN-100;
exposure time, 300
hours.

(c) CoCrAlY coated VIA;
exposure time, 180
hours.

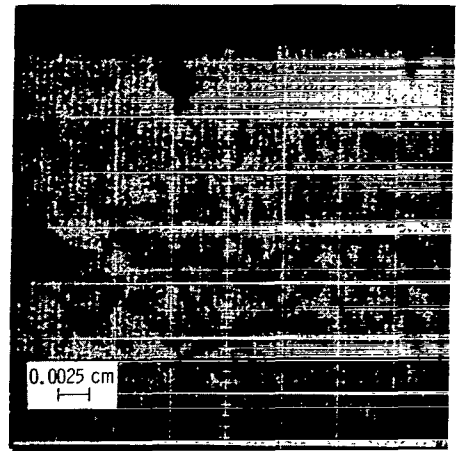
(d) CoCrAlY coated VIA;
exposure time, 600
hours.

Figure 10. - CoCrAlY coated IN-100 and VIA alloy specimens after high-velocity gas cyclic oxidation at 1093° C (2000° F) using 1 hour cycles.

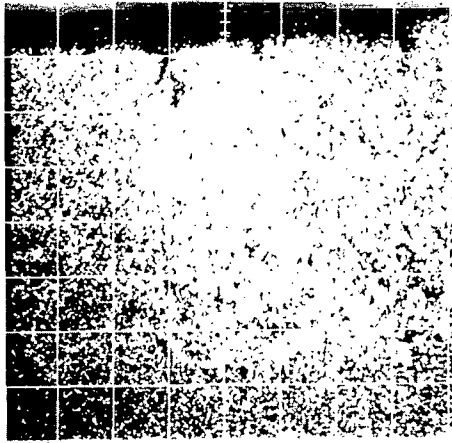


Light micrograph (light etch)

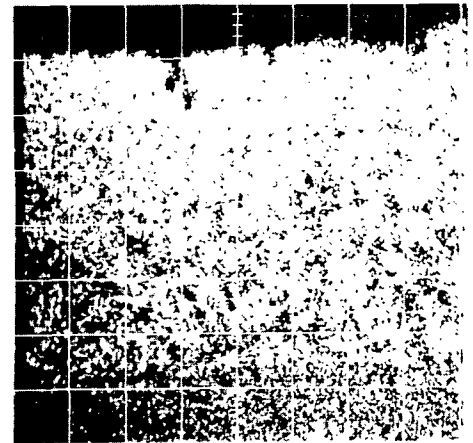
$\alpha\text{Al}_2\text{O}_3$
 Co(ss)
 $\beta(\text{CoAl})$, Co(ss)
 and Ti-Mo
 monocarbides
 Substrate



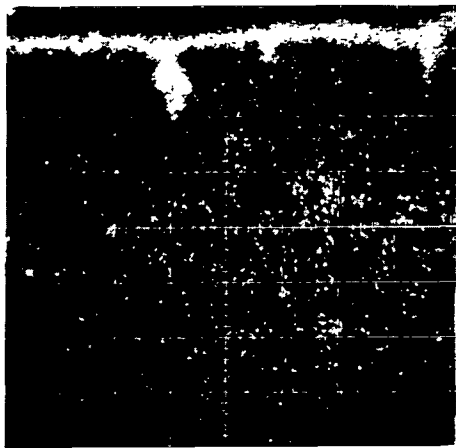
Electron backscatter image



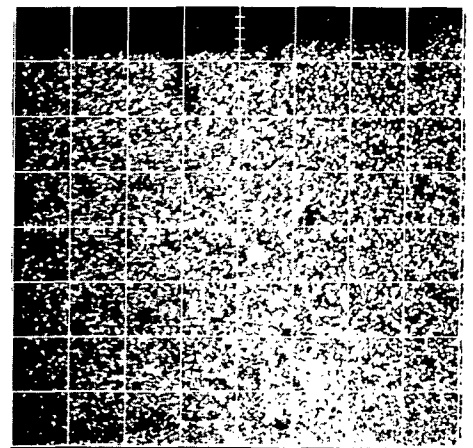
Cobalt image



Chromium image

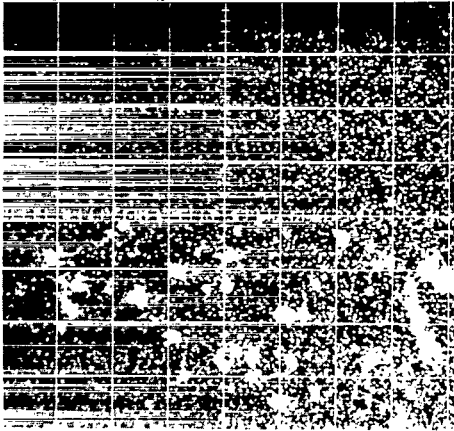


Aluminum image

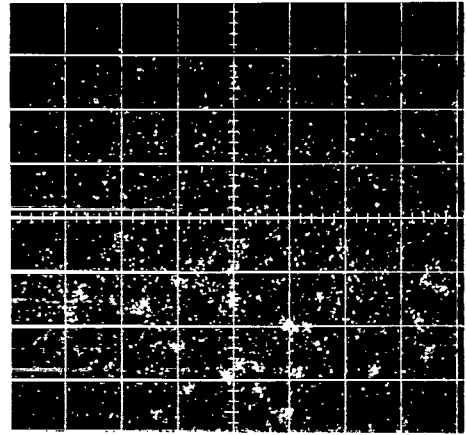


Nickel image

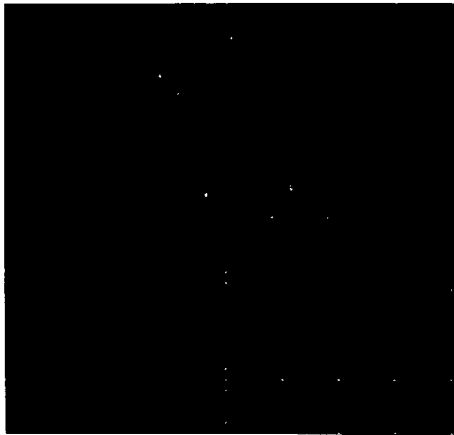
Figure 11. - Element distribution in CoCrAlY coated IN-100 alloy after 300 hours at 1093° C (2000° F) using electron microprobe.



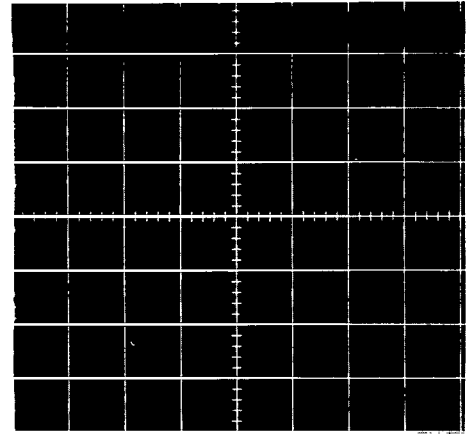
Titanium image



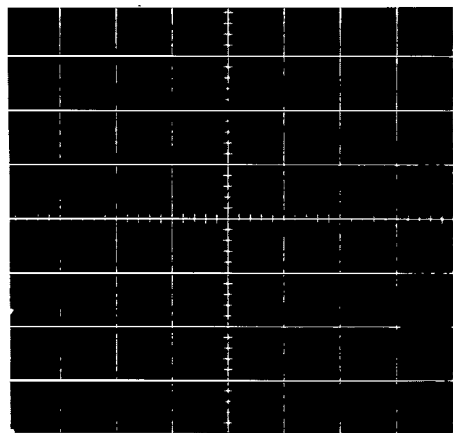
Molybdenum image



Yttrium image



Tantalum image



Tungsten image

Figure 11. - Concluded.



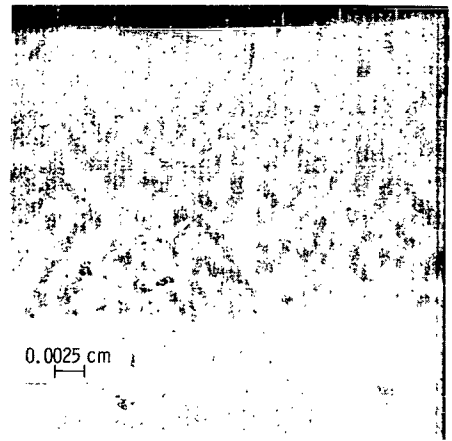
==== $\alpha\text{Al}_2\text{O}_3, \text{Y}_4\text{Al}_2\text{O}_9$

Co(ss)

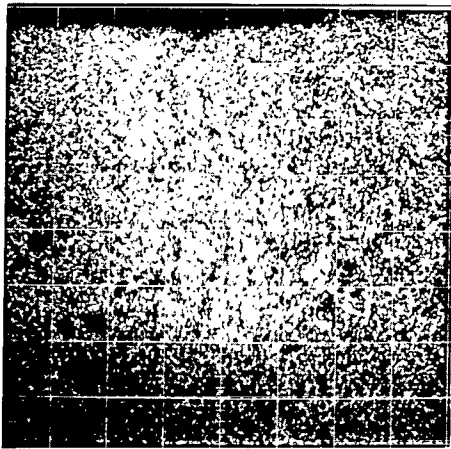
β(CoAl), Co(ss)
carbides of Ta
and Ti

Substrate

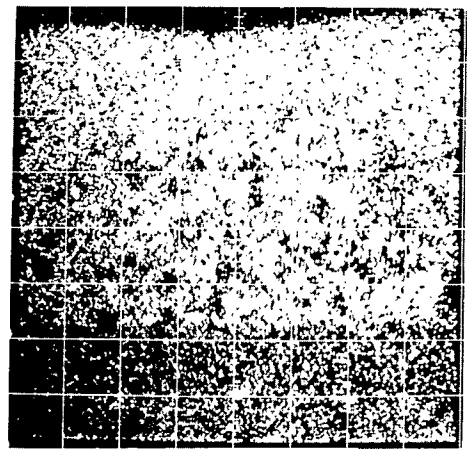
Light micrograph (light etch)



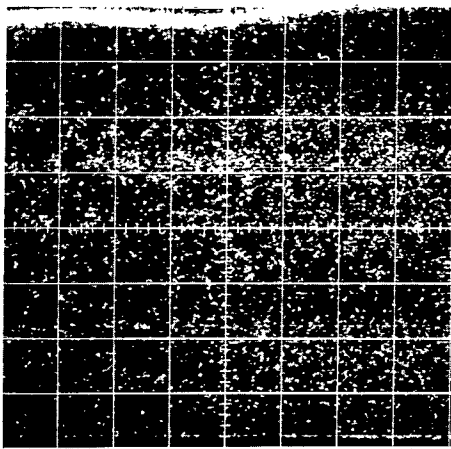
Electron backscatter image



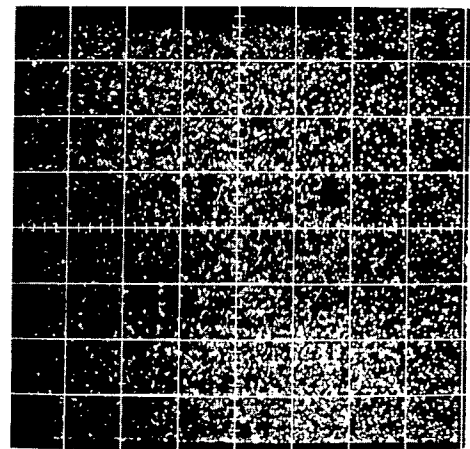
Cobalt image



Chromium image

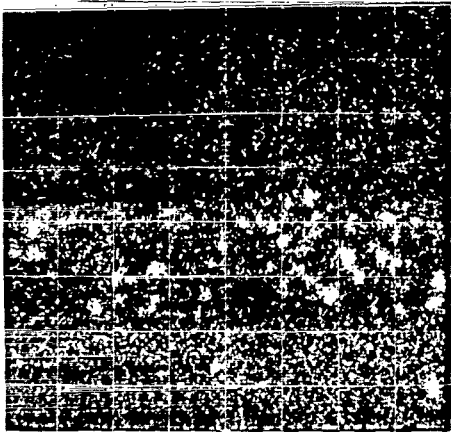


Aluminum image

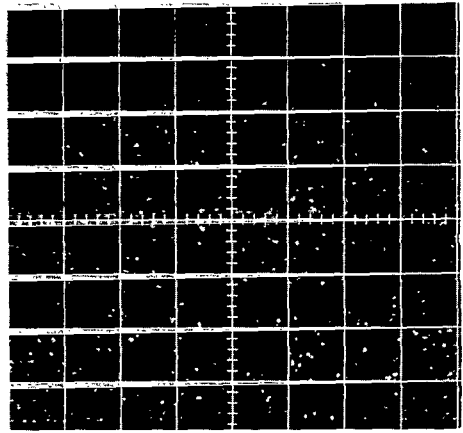


Nickel image

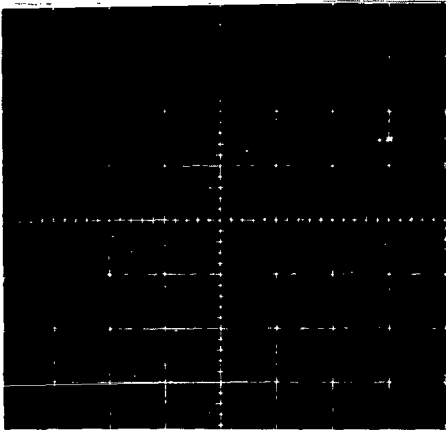
Figure 12. - Element distribution in CoCrAlY coated VIA alloy after 600 hours at 1093° C (2000° F) using electron microprobe.



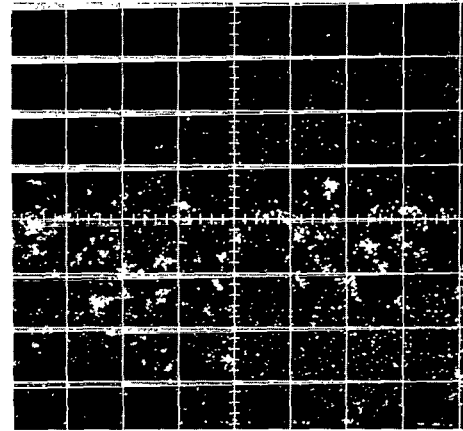
Titanium image



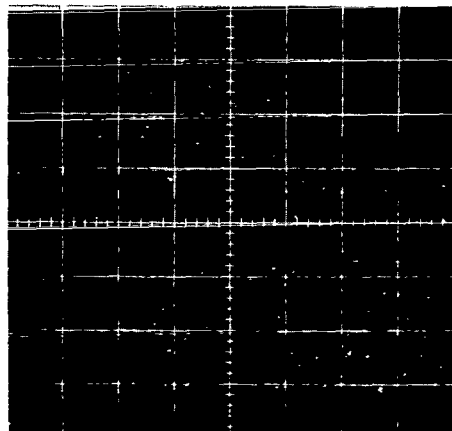
Molybdenum image



Yttrium image

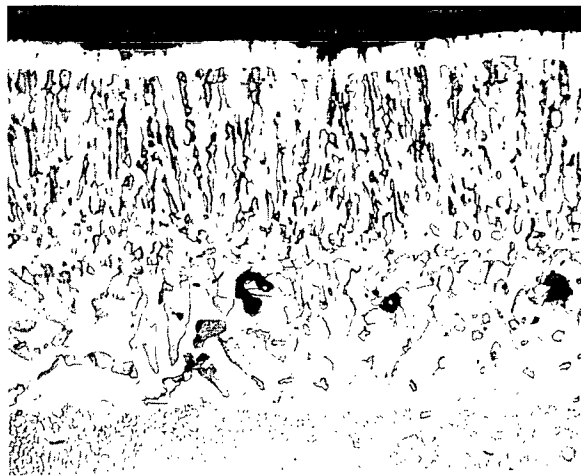


Tantalum image



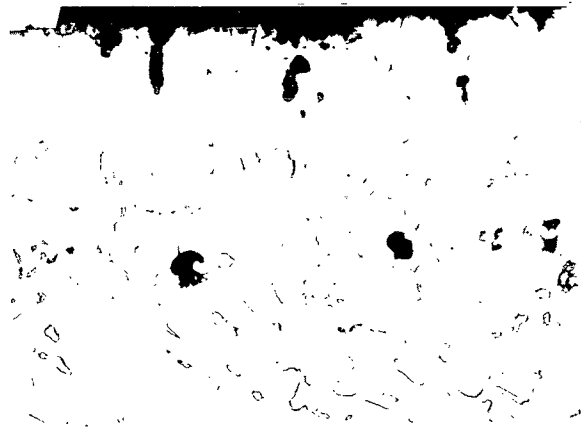
Tungsten image

Figure 12. - Concluded.



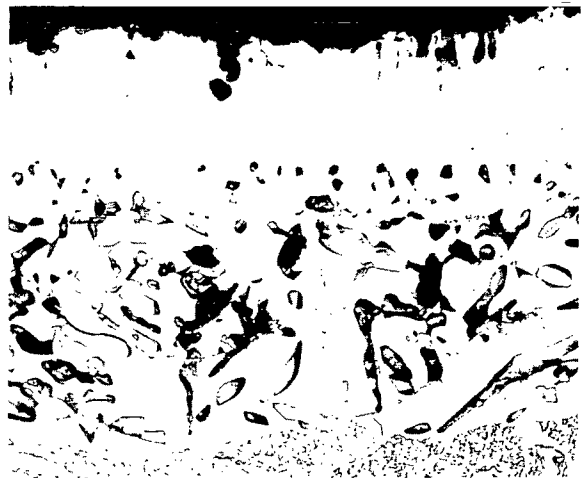
$\alpha\text{Al}_2\text{O}_3$
 Co(ss)
 $\beta(\text{CoAl}), \text{Co(ss)}$
 $\beta(\text{CoAl})$ and Ti-Mo
 monocarbide particles
 in Co(ss) matrix
 Substrate

(a) Cyclic oxidation, 100 hours.



Co(ss);
 340 DPH
 $\beta(\text{CoAl})$ and Ti-Mo
 monocarbide particles
 in Co(ss) matrix;
 420 DPH
 ----- 450 DPH

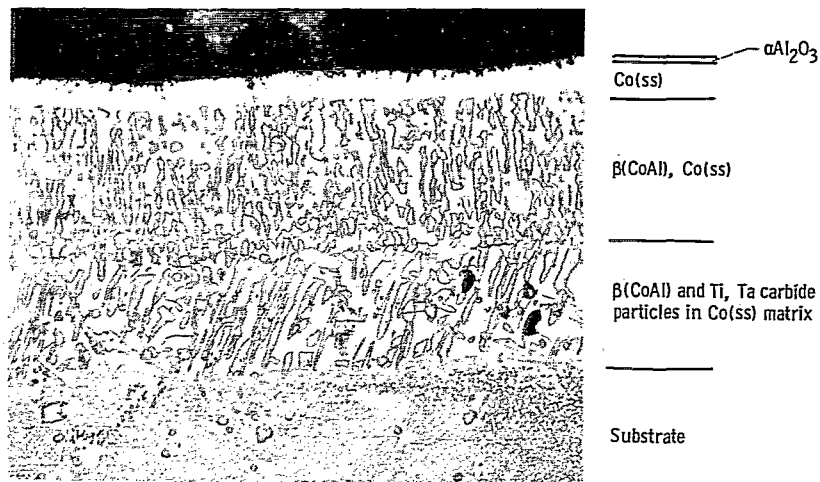
(b) Cyclic oxidation, 300 hours; light etch.



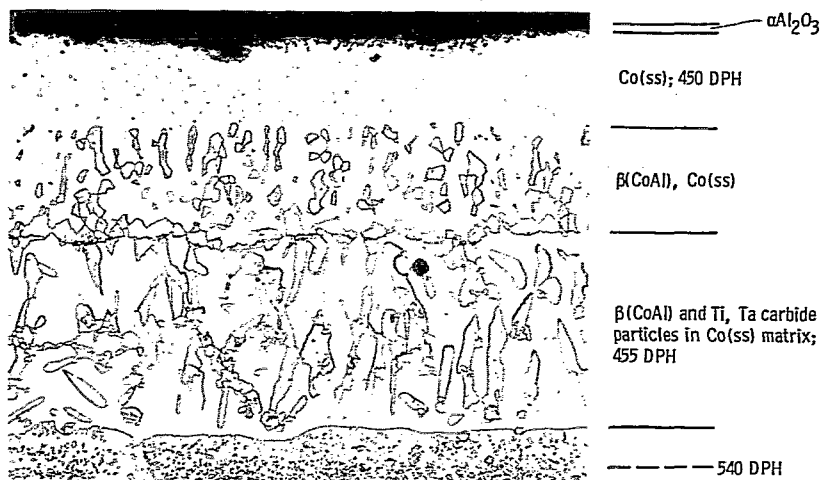
0.0025 cm
 ───┬───

(c) Cyclic oxidation, 300 hours; heavy etch.

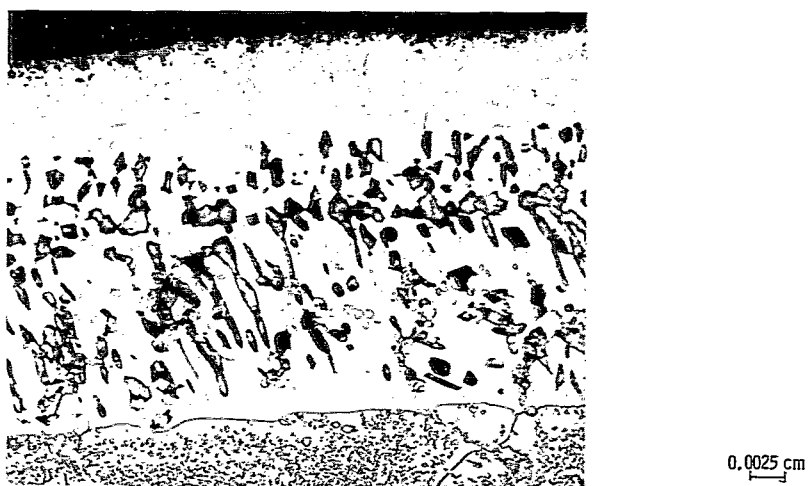
Figure 13. - Microstructures of CoCrAlY coated IN-100 after cyclic oxidation at 1093° C (2000° F) in high-velocity gas. (DPH denotes diamond pyramid hardness.)



(a) Cyclic oxidation, 100 hours.

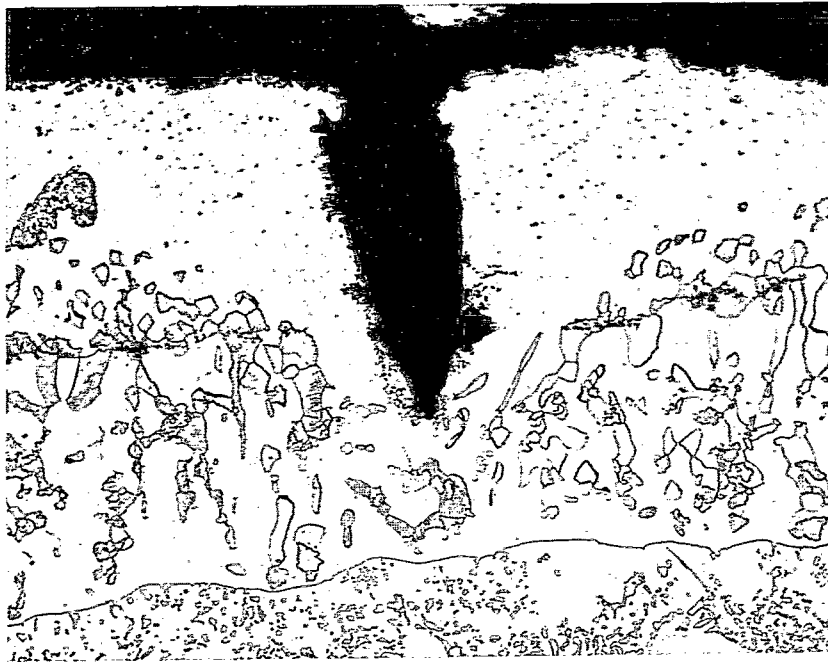


(b) Cyclic oxidation, 600 hours; light etch.



(c) Cyclic oxidation, 600 hours; heavy etch.

Figure 14. - Microstructures of CoCrAlY coated VIA alloy after cyclic oxidation at 1093° C (2000° F) in high-velocity gas. (DPH denotes diamond pyramid hardness.)



0.0025 cm

Figure 15. - Cross section of a surface pit formed on CoCrAlY coated VIA alloy after 600 hours cyclic oxidation at 1093° C (2000° F) in high-velocity gas. Light etch.



NASA 451

012 001 C1 U 17 720714 S00903DS
DEPT OF THE AIR FORCE
AF WEAPONS LAB (AFSC)
TECHNICAL LIBRARY/DOUL/
ATTN: E LOU BOWMAN, CHIEF
KIRTLAND AFB NM 87117

POSTMASTER: If Undeliverable (Section 158
Postal Manual) Do Not Return

"The aeronautical and space activities of the United States shall be conducted so as to contribute . . . to the expansion of human knowledge of phenomena in the atmosphere and space. The Administration shall provide for the widest practicable and appropriate dissemination of information concerning its activities and the results thereof."

— NATIONAL AERONAUTICS AND SPACE ACT OF 1958

NASA SCIENTIFIC AND TECHNICAL PUBLICATIONS

TECHNICAL REPORTS: Scientific and technical information considered important, complete, and a lasting contribution to existing knowledge.

TECHNICAL NOTES: Information less broad in scope but nevertheless of importance as a contribution to existing knowledge.

TECHNICAL MEMORANDUMS: Information receiving limited distribution because of preliminary data, security classification, or other reasons.

CONTRACTOR REPORTS: Scientific and technical information generated under a NASA contract or grant and considered an important contribution to existing knowledge.

TECHNICAL TRANSLATIONS: Information published in a foreign language considered to merit NASA distribution in English.

SPECIAL PUBLICATIONS: Information derived from or of value to NASA activities. Publications include conference proceedings, monographs, data compilations, handbooks, sourcebooks, and special bibliographies.

TECHNOLOGY UTILIZATION PUBLICATIONS: Information on technology used by NASA that may be of particular interest in commercial and other non-aerospace applications. Publications include Tech Briefs, Technology Utilization Reports and Technology Surveys.

Details on the availability of these publications may be obtained from:

SCIENTIFIC AND TECHNICAL INFORMATION OFFICE

NATIONAL AERONAUTICS AND SPACE ADMINISTRATION

Washington, D.C. 20546